

Zgoubi-ing AGS : spin motion with snakes and jump-quads,  $G = 43.5$   
through  $G = 46.5$  and beyond

F. Meot,

October 2009

Collider Accelerator Department  
**Brookhaven National Laboratory**

**U.S. Department of Energy**

USDOE Office of Science (SC)

Notice: This technical note has been authored by employees of Brookhaven Science Associates, LLC under Contract No. DE-AC02-98CH10886 with the U.S. Department of Energy. The publisher by accepting the technical note for publication acknowledges that the United States Government retains a non-exclusive, paid-up, irrevocable, world-wide license to publish or reproduce the published form of this technical note, or allow others to do so, for United States Government purposes.

## **DISCLAIMER**

This report was prepared as an account of work sponsored by an agency of the United States Government. Neither the United States Government nor any agency thereof, nor any of their employees, nor any of their contractors, subcontractors, or their employees, makes any warranty, express or implied, or assumes any legal liability or responsibility for the accuracy, completeness, or any third party's use or the results of such use of any information, apparatus, product, or process disclosed, or represents that its use would not infringe privately owned rights. Reference herein to any specific commercial product, process, or service by trade name, trademark, manufacturer, or otherwise, does not necessarily constitute or imply its endorsement, recommendation, or favoring by the United States Government or any agency thereof or its contractors or subcontractors. The views and opinions of authors expressed herein do not necessarily state or reflect those of the United States Government or any agency thereof.

# **Zgoubi-ing AGS: spin motion with snakes and jump-quads, $G\gamma = 43.5$ through $G\gamma = 46.5$ and beyond**

**F. Meot, L. Ahrens, J. Glenn, H. Huang,  
A. Luccio, W. W. MacKay, T. Roser, N. Tsoupas**

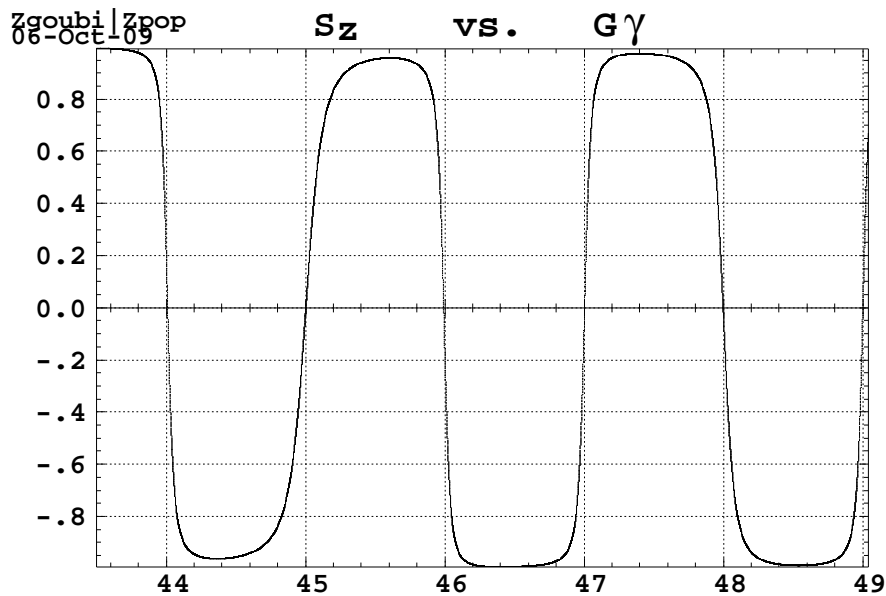


**Collider-Accelerator Department  
Brookhaven National Laboratory  
Upton, NY 11973**

Notice: This document has been authorized by employees of Brookhaven Science Associates, LLC under Contract No. DE-AC02-98CH10886 with the U.S. Department of Energy. The United States Government retains a non-exclusive, paid-up, irrevocable, world-wide license to publish or reproduce the published form of this document, or allow others to do so, for United States Government purposes.

**Zgoubi-ing AGS : spin motion with snakes and jump-quads,**  
 $G\gamma = 43.5 \rightarrow G\gamma = 46.5$  and beyond

A work performed at BNL in October and December 2009, in collaboration with  
 L. Ahrens, J. Glenn, H. Huang, A. Luccio, W. W. MacKay, T. Roser, N. Tsoupas



## Abstract

This Note reports on the first, and successful, simulations of particle and spin dynamics in the AGS in presence of the two helical snakes and of the tune-jump quadrupoles, using the ray-tracing code Zgoubi.

It includes DA tracking in the absence or in the presence of the two helical snakes, simulation of particle and spin motion in the snakes using their magnetic field maps, spin flipping at integer resonances in the  $36+Q_y$  depolarizing resonance region (Figure above), with and without tune-jump quadrupole gymnastics. It also includes details on the setting-up of Zgoubi input data files and on the various numerical methods of concern in and available from Zgoubi.

This work is a follow-on of C-AD/AP/452.

## Contents

<b>1</b>	<b>Introduction</b>	<b>3</b>
<b>2</b>	<b>Lattice</b>	<b>3</b>
2.1	Paraxial parameters . . . . .	3
2.2	Spin $\vec{n}$ -vector . . . . .	5
2.3	Large amplitude motion . . . . .	7
<b>3</b>	<b>W and C snakes, <math>E = 43.5M_0/G</math></b>	<b>9</b>
<b>4</b>	<b>Spin tracking, <math>\gamma G = 43.5 \rightarrow 49</math></b>	<b>10</b>
4.1	Zero emittance . . . . .	10
4.2	Non-zero horizontal emittance . . . . .	13
<b>5</b>	<b>Spin tracking, <math>\gamma G = 43.5 \rightarrow 49</math>, including Q-jump</b>	<b>15</b>
	<b>Appendix</b>	<b>24</b>
<b>A</b>	<b>MAD files</b>	<b>24</b>
A.1	Command file . . . . .	24
A.2	“dipole1” file . . . . .	25
A.3	“print” file . . . . .	26
<b>B</b>	<b>Zgoubi data file specimen</b>	<b>27</b>
B.1	1-turn first order mapping, input file . . . . .	27
B.2	Acceleration, using “CAVITE” . . . . .	27
B.3	zgoubi.dat for w- and c-snake . . . . .	27
B.4	Spin $\vec{n}$ -vector . . . . .	28
B.5	Q-jump . . . . .	28

## 1 Introduction

AGS with  $\nu_x / \nu_y = 8.72 / 8.98$  is tracked in presence of the Warm and Cold snakes, with or without tune-jump quadrupoles.

The report describes paraxial and large amplitude properties of the lattice, with snakes as well as without snakes when useful for comparison. A dedicated section addresses the properties of the snakes themselves, as drawn from ray-tracing using their OPERA magnetic field maps. Depolarizing resonance crossing and spin flipping, as well as effects of the tune-jump quadrupoles, are explored by accelerating from  $\gamma G = 43.5$  to  $\gamma G = 46.5$ .

Table 1: AGS parameters from MAD8 (left col.), from Zgoubi “Brute from MAD8” without snakes (middle col.) and with warm and cold snakes (rightmost col.).

		MAD8 no snake	Ray-tracing Brute from MAD8 <sup>1</sup>	
			without snake	with w & c snakes
$\gamma G$		non relevant	non relevant	43.5
Closed orbit length	(m)	807.075652 <sup>2</sup>	807.04275 <sup>3</sup>	807.04274
Qx, Qy		8.7200, 8.9800	[8].72132, [8].97774	[8].73016, [8].97827 <sup>(4,5)</sup>
Q'x, Q'y		-22.4703, 2.6985	-22.5430, 2.6059	-24.844, 2.8446
$\alpha, \sqrt{1/\alpha}$		0.01390, 8.4829	0.0139, 8.470	0.01388, 8.4867
<i>Periodic functions at entrance to “AIBF” :</i>				
$\beta_x, \beta_y$	(m)	19.455, 9.682	19.583, 10.241	19.436, 10.036
$\alpha_x, \alpha_y$		-1.537, 0.808	-1.550, 0.865	-1.524, 0.843
$D_x, D'_x$	(m,-)	1.990, 0.120	1.977, 0.123	2.029, 0.126
$D_y, D'_y$	(m,-)	0, 0	0, 0	0.256, 0.0245
H closed orbit <sup>(2)</sup> , $x_{co}, x'_{co}$	mm, mrad	0, 0	-6.110, -0.413	-5.834, -0.413
V closed orbit <sup>(2)</sup> , $y_{co}, y'_{co}$	mm, mrad	0, 0	0, 0	-1.863, -0.087

(1) All magnets hard-edge, lack of  $B_s$  integral in bends is compensated by vertical kick  $\delta y' = y * (-\tan(\text{wedge}) + FFL/(6.D0 * \rho * \cos(\text{wedge})))$  with FFL=0 here following MAD data - taking  $FFL \approx \text{gap}$  in Zgoubi changes  $\nu_y$  by  $\approx -10^{-3}$ .

Integration step size in Zgoubi : (i) 1 cm in the snakes, (ii) 40 steps in the main dipoles.

(2) MAD uses 'SBEND' for main bends, see App. A.2.

(3) The difference in orbit lengths here arises from the treatment of the closed orbit. The actual theoretical length is 807.09 m, see footnote.

(4) Data obtained from first order mapping.

(5) Data obtained from multiturn and Fourier analysis.

## 2 Lattice

### 2.1 Paraxial parameters

The left column in Tab. 1 displays the general optical parameters of AGS bare lattice as obtained from MAD8, without snake. Details concerning respectively MAD input/output data can be found in App. A.1/App. A.3.

Zgoubi input optics file (so-called “zgoubi.dat”) is obtained by translation from MAD8 “survey” type of output or MADX “twiss” type of output (an automatic translator is available). Parameter values so obtained with the bare lattice are given in the middle column in Tab. 1 for comparison with MAD ones. Sample zgoubi.dat can be found in Apps. B.1. Note that both Zgoubi and MAD sets of orbit as well as first and second order parameter values have later been brought to very good agreement<sup>1</sup>.

<sup>1</sup>(i) The  $\approx 3.2$  cm difference in orbit length arises from the treatment of the reference closed orbit which does not coincide with the

The rightmost column in Tab. 1 gives machine parameters in presence of the two snakes at  $\gamma G = 43.5$ , snakes' characteristics are addressed in Sec. 3.

Horizontal and vertical closed orbits in the presence of the snakes are shown in Fig. 1.

Table 2: A list of the depolarizing resonances in the range  $43 \leq \gamma G \leq 47$  and beyond.  $\nu_x = 8.7302$ ,  $\nu_z = 8.9783$ .

---

Imperfection resonances			
	$\gamma G$	T	$B\rho$
	43	21.56543	74.99899
	44	22.08877	76.74614
	45	22.61211	78.49324
	46	23.13545	80.24029
	47	23.65879	81.98726
	48	24.18213	83.73419
	49	24.70548	85.48106
	50	25.22882	87.22788
	51	25.75216	88.97466

Intrinsic resonances			
$M \pm \nu_z$	$G\gamma$	T	$B\rho$
52- $\nu_z$	43.02170	21.57678	75.03689
35+ $\nu_z$	43.97830	22.07741	76.70824
53- $\nu_z$	44.02170	22.10012	76.78407
36+ $\nu_z$	44.97830	22.60075	78.45534
54- $\nu_z$	45.02170	22.62346	78.53116
37+ $\nu_z$	45.97830	23.12410	80.20238
55- $\nu_z$	46.02170	23.14680	80.27818
38+ $\nu_z$	46.97830	23.64744	81.94936
56- $\nu_z$	47.02170	23.67015	82.02516

Intrinsic resonances, coupled			
$M \pm \nu_x$			
52 - $\nu_x$	43.26980	21.70662	75.47037
35 + $\nu_x$	43.73020	21.94757	76.27477
53 - $\nu_x$	44.26980	22.22996	77.21751
36 + $\nu_x$	44.73020	22.47091	78.02188
54 - $\nu_x$	45.26980	22.75331	78.96460
37 + $\nu_x$	45.73020	22.99425	79.76894
55 - $\nu_x$	46.26980	23.27665	80.71162
38 + $\nu_x$	46.73020	23.51760	81.51594

---

“Optimum Closed Orbit” (so-called “OCO”), in the present work. The theoretical length of the OCO is 807.09 m, this has been settled in further works, see PAC and IPAC Conference papers, 2010, 2011. (ii) Details on the numerical results and the agreement between MAD and Zgoubi, as long as both codes are given input data that describe the same optics (regardless of the ability of matrix-formalism type of input data to accurately model the real AGS), can be found in IPAC and PAC publications, 2010, 2011

## 2.2 Spin $\vec{n}$ -vector

The spin precession  $\vec{n}$ -axis is obtained from the ray-tracing by FIT-ting (getting identical) final and initial spin coordinates for the ideal particle (travelling on the on-momentum closed orbit).

The corresponding zgoubi.dat are given in App. B.4.



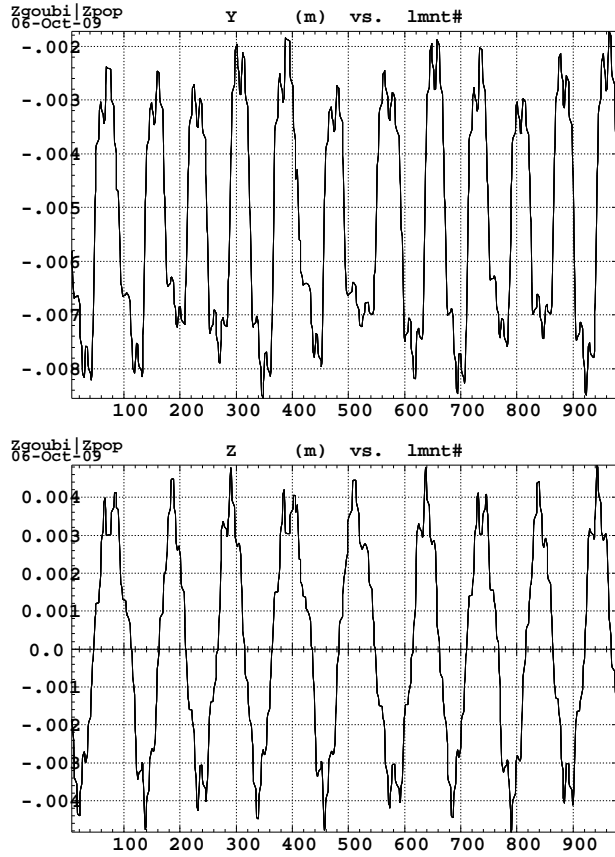


Figure 1: H and V closed orbits in presence of w- and c-snake, recorded at  $\sim 990$  different locations along the ring circumference. (closed orbits have later been brought to zero, based on introducing the OCO in Zgoubi data - see footnote page 1.)

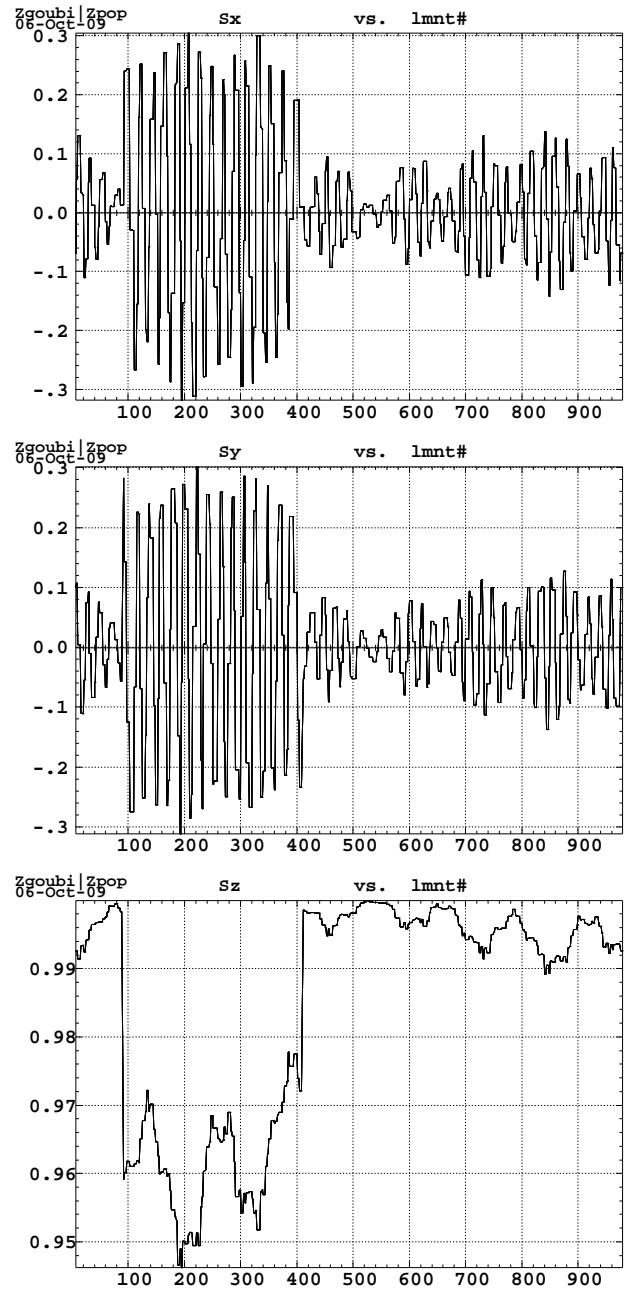


Figure 2: Components of the spin  $\vec{n}$ -axis in presence of w- and c-snake, as recorded at  $\sim 990$  locations along the ring circumference.

### 2.3 Large amplitude motion

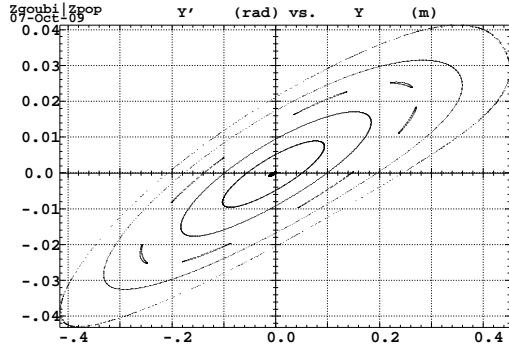
Integration step size in the following is 1 mm in w- and c-snake 2-D field maps and about 5 cm in main dipoles.

#### Dynamic aperture in the $\nu_y = 8.98$ bare lattice, no snake

The phase-space portraits in Figs. 3,4 show the maximum stable amplitudes together with intermediate invariants, in the bare lattice without snake (conditions of the middle column in Tab. 1, “ray-tracing, without snake”).

Amplitude detuning is shown next to the plots.

Dynamic aperture is shown in Fig. 5.



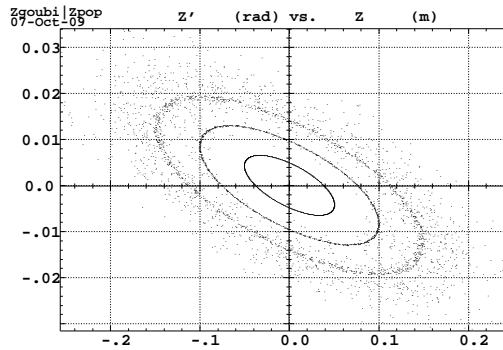
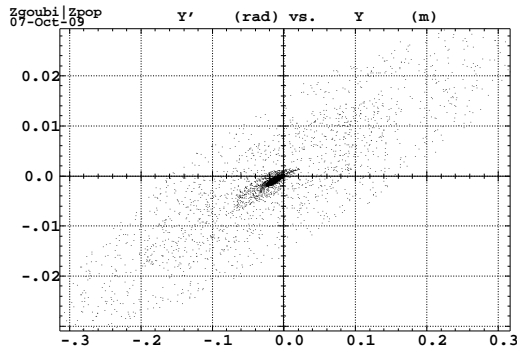
Detuning, from smaller to larger H-amplitude :

Qx	Qy	paraxial
7.212472	9.778009	
7.017703		
6.521219		
5.713944		
5.327142		
7.270152		

Figure 3: 1000-turn maximum stable amplitudes without snake.

Six H invariants ranging from  $\sim 0$  to stability limit launched with  $\epsilon_y = 0$  (left).

V motion is zero, no  $H \rightarrow V$  coupling.



Detuning, from smaller to larger V-amplitude :

Qx	Qy	paraxial
0.7254081	0.9770309	
0.7272465	0.9742884	
0.7322278	0.9671178	
0.7407944	0.9558546	
0.7527732	0.9414990	
0.7513091	0.9361446	

Figure 4: 1000-turn maximum stable amplitudes without snake.

Six V invariants ranging from  $\sim 0$  to stability limit launched with  $\epsilon_x = 0$  (right) ; induced H motion

(left).

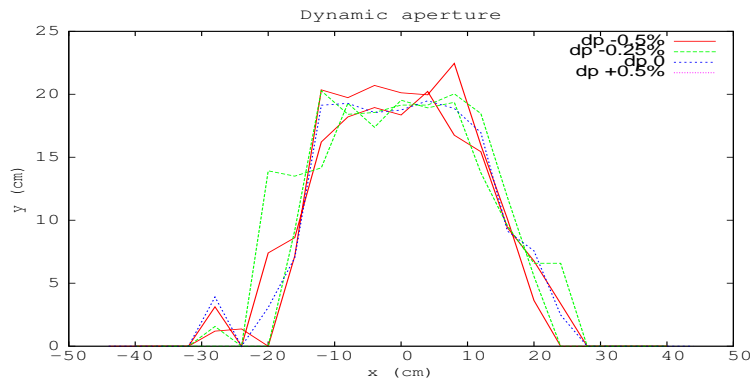


Figure 5: Dynamic apertures without snake.

**Dynamic aperture in presence of w- and c-snake,  $E = 43.5M_0/G$**

The phase-space portraits in Figs. 6,7 show the maximum stable amplitudes together with intermediate invariants (conditions of the rightmost column in Tab. 1, “ray-tracing, with w & c snakes”). Coupling induces substantial motion from  $x$  into  $y$ , and reciprocally.

Amplitude detuning is shown next to the plots.

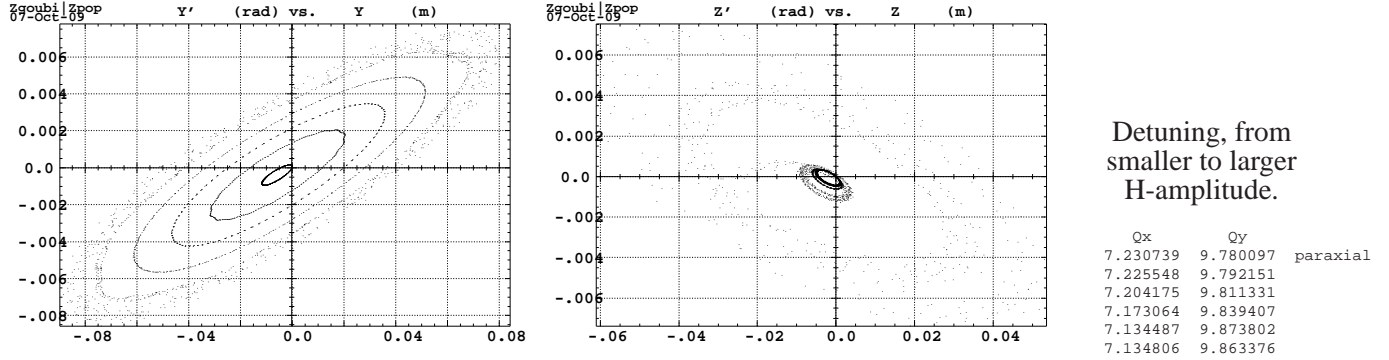


Figure 6: 1000-turn maximum stable amplitudes in presence of w- and c-snake. Six H invariants ranging from  $\sim 0$  to stability limit launched with  $\epsilon_y = 0$  (left) ; induced V motion (right).

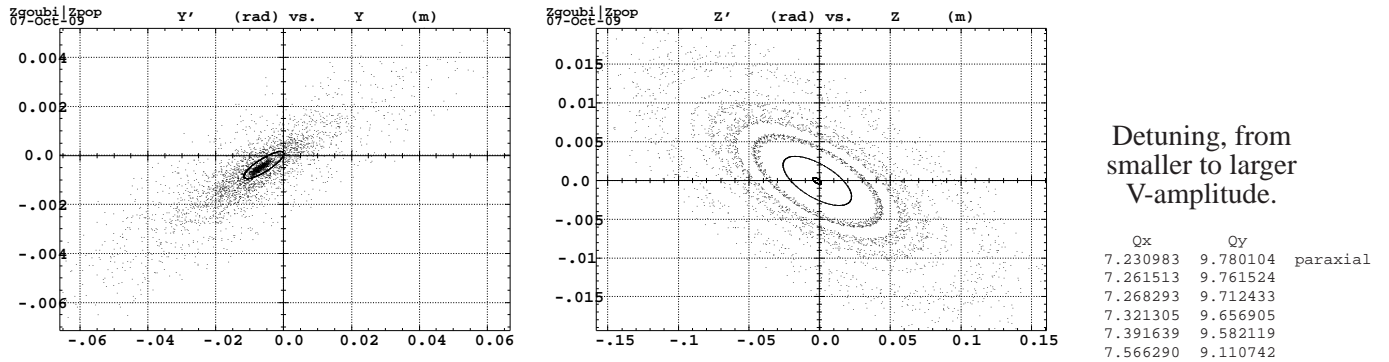


Figure 7: 1000-turn maximum stable amplitudes in presence of w- and c-snake. Six V invariants ranging from  $\sim 0$  to stability limit launched with  $\epsilon_x = 0$  (right) ; induced H motion (left).

Dynamic aperture in presence of the snakes is shown in Fig. 8. Comparison with DA in the bare lattice without snake, Fig. 5, shows that these have a substantial effect.

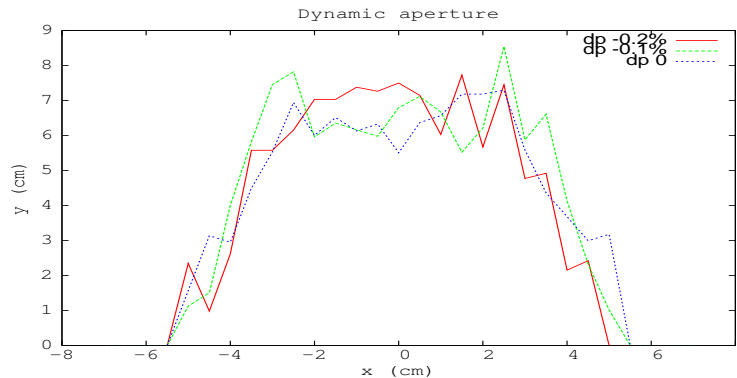


Figure 8: Dynamic apertures in presence of w- and c-snake, for  $\delta p/p = 0, \pm 0.1\%, \pm 0.2\%$ , 5 mm step in  $x$ , 1 mm precision on vertical boundary.

### 3 W and C snakes, $E = 43.5M_0/G$

Basic behavior of magnetic field and of particle and spin motion in w- and c-snake is checked.

W-snake is represented by the 3-D field map “table55.tab”. In the AGS lattice file zgoubi.dat, it is encompassed within two negative 0.5 m drifts so to fit into the 3 meters space allotted. C-snake is represented by the 3-D field map “ref+sole.tab”. Tracking in Zgoubi is performed using the “TOSCA” procedure ; input data files can be found in App. B.3.

Field components, particle motion and spin motion, along w-snake, are represented in Fig. 9. C-snake ones are represented in Fig. 10.

When used in the ring, W-snake field has the strength shown in Fig. 9, C-snake field has a strength attenuated by 0.7 compared to Fig. 10. Note that for multiturn tracking reported in the other Sections in this paper, mid-plane 2-D field maps extracted from respectively “table55.tab” “ref+sole.tab” are used rather than the 3-D ones, this yields as good results and has the merit of much smaller data volume, faster reading.

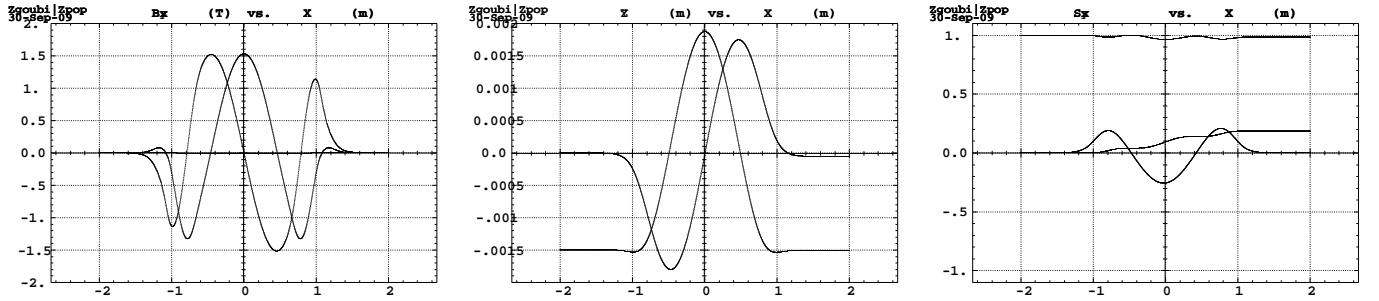


Figure 9: Warm snake, particle with  $\gamma G = 43.5$  launched in “table55.tab” with  $x=-1.5$  mm,  $y=0$ ,  $x'=y'=0$ .  $B_x, B_y, B_z$  (left),  $x, y$  (middle) and  $S_x, S_y, S_z$  (right).

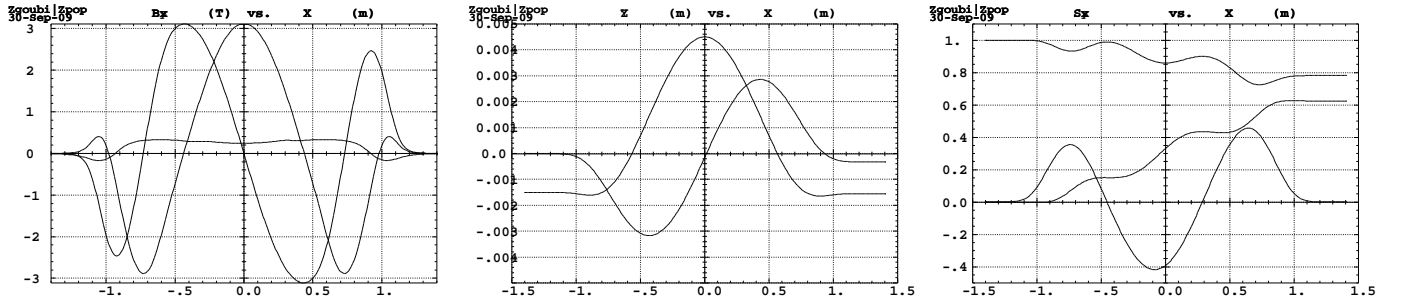


Figure 10: Cold snake with solenoid, particle with  $\gamma G = 43.5$  launched in “ref+sole.tab” with  $x=-1.5$  mm,  $y=0$ ,  $x'=y'=0$ .  $B_x, B_y, B_z$  (left),  $x, y$  (middle) and  $S_x, S_y, S_z$  (right).

## 4 Spin tracking, $\gamma G = 43.5 \rightarrow 49$

**How long that takes :**  $\sim 0.15$  second per turn, *real time*, on a DELL Latitude D630 laptop, hence  $\sim 50$  min. for the present 20000-turn run<sup>2</sup>.

Working hypothesis in the numerical simulations are the following (see zgoubi.dat in App. B.2).

Total potential  $\hat{V} = 290$  kV

Synchronous phase  $\phi_s = 150$  degrees

hence energy gain  $\Delta E = 145$  keV/turn, then, given  $M_0 = 938.27203$  MeV,  $G = 1.7928474$

$$\alpha = G \frac{d\gamma}{d\theta} = G \frac{1}{2\pi} \frac{\Delta E}{M_0}$$

$$\alpha = 4.4096356 \cdot 10^{-5}$$

Besides,

$$\dot{B} = \Delta E / (2\pi R\rho) = \Delta E / (C\rho)$$

Given

$$C = 807.043 \text{ m (Tab. 1)}$$

and  $1/\rho = B/B\rho = 0.0117125$ , cf. dipole component in 'SBEN' type of magnets, zgoubi.dat file in App. B.1

(Note :  $\rho = 85.3785$ , packing factor  $R/\rho = 9.45254$ ), then

$$\dot{B} = 2.104 \text{ T/s}$$

Acceleration from  $\gamma G = 43.5$  to  $\gamma G = 46$  requires  $\sim 10000$  turns, the experiment is pushed to 20000 turns and  $\gamma G = 49$ . Resonances in that energy region are given in Tab. 2, all imperfection resonances but for  $\gamma G = 36 + \nu_z \approx 44.98$ .

### 4.1 Zero emittance

We consider  $\epsilon_x$  and  $\epsilon_y \approx 0$  in this Section.

Spin tracking results are shown in Fig. 11.

Fig. 12 allows monitoring (correctness of) particle dynamics, it can be observed that the particle stays near H and V closed orbits and synchronous phase over the 20000 turns.

<sup>2</sup>For comparison with SPINK : following talks at spin meeting on Oct. 2nd, SPINK takes about 10 hours for  $6 \cdot 10^5$  turns

$S_x, S_y, S_z$  versus  $G\gamma$ , for  $\epsilon_x$  and  $\epsilon_y \approx 0$

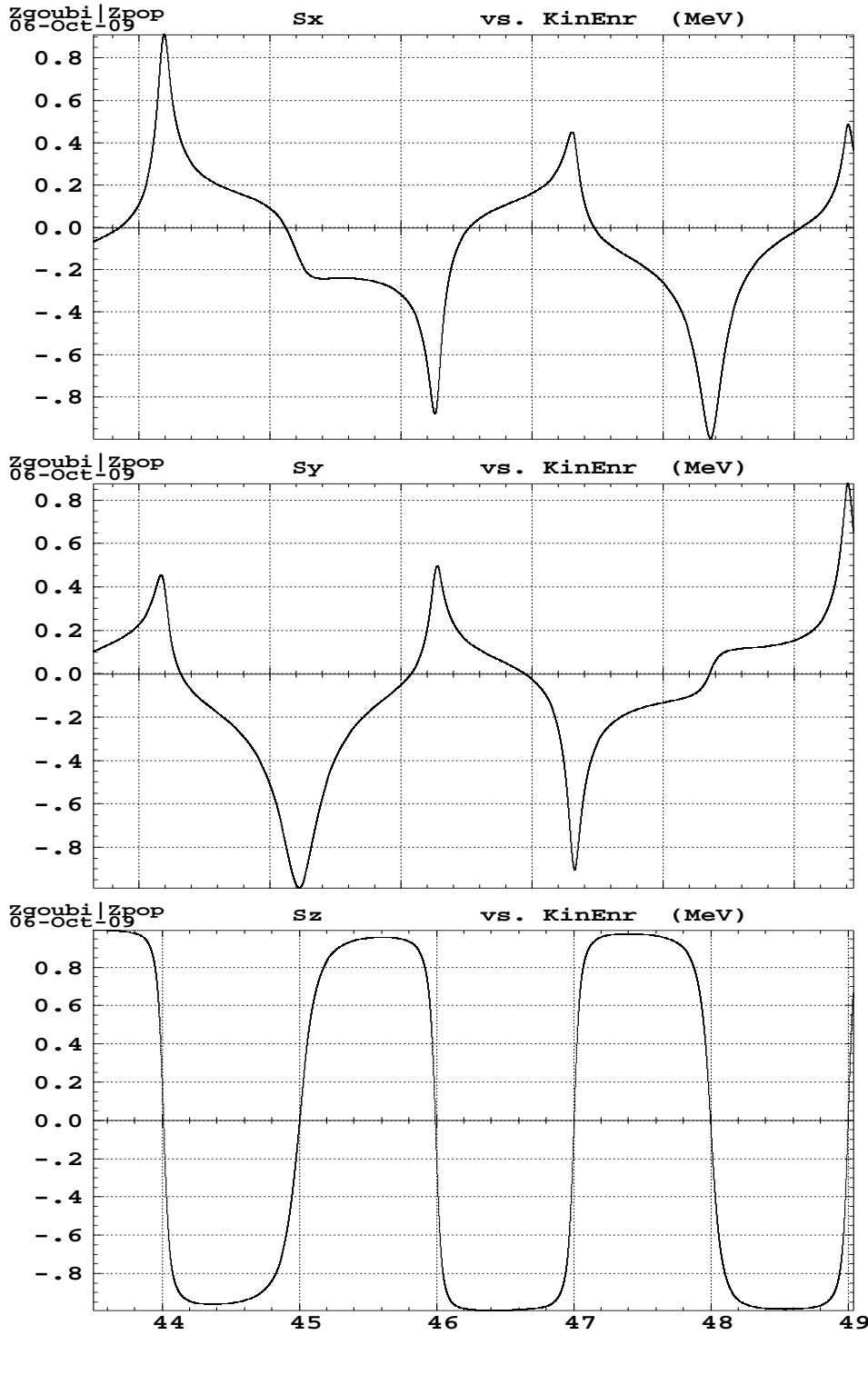


Figure 11: Spin motion experienced by the synchronous particle in presence of w- and c-snake, over  $G\gamma : 43.5 \rightarrow 49$ .

The figure shows the spin components  $S_x$  (longitudinal),  $S_y$  (radial),  $S_z$  (vertical) (from top to bottom) observed in an arc over 20000 turns.

The two smaller boxes, lower-right, zoom on the fine structure : initial  $S_z$  over the first 200 turns (top box) and  $S_z$  over 200 turns in  $\gamma G = 47.5$  region (bottom box)

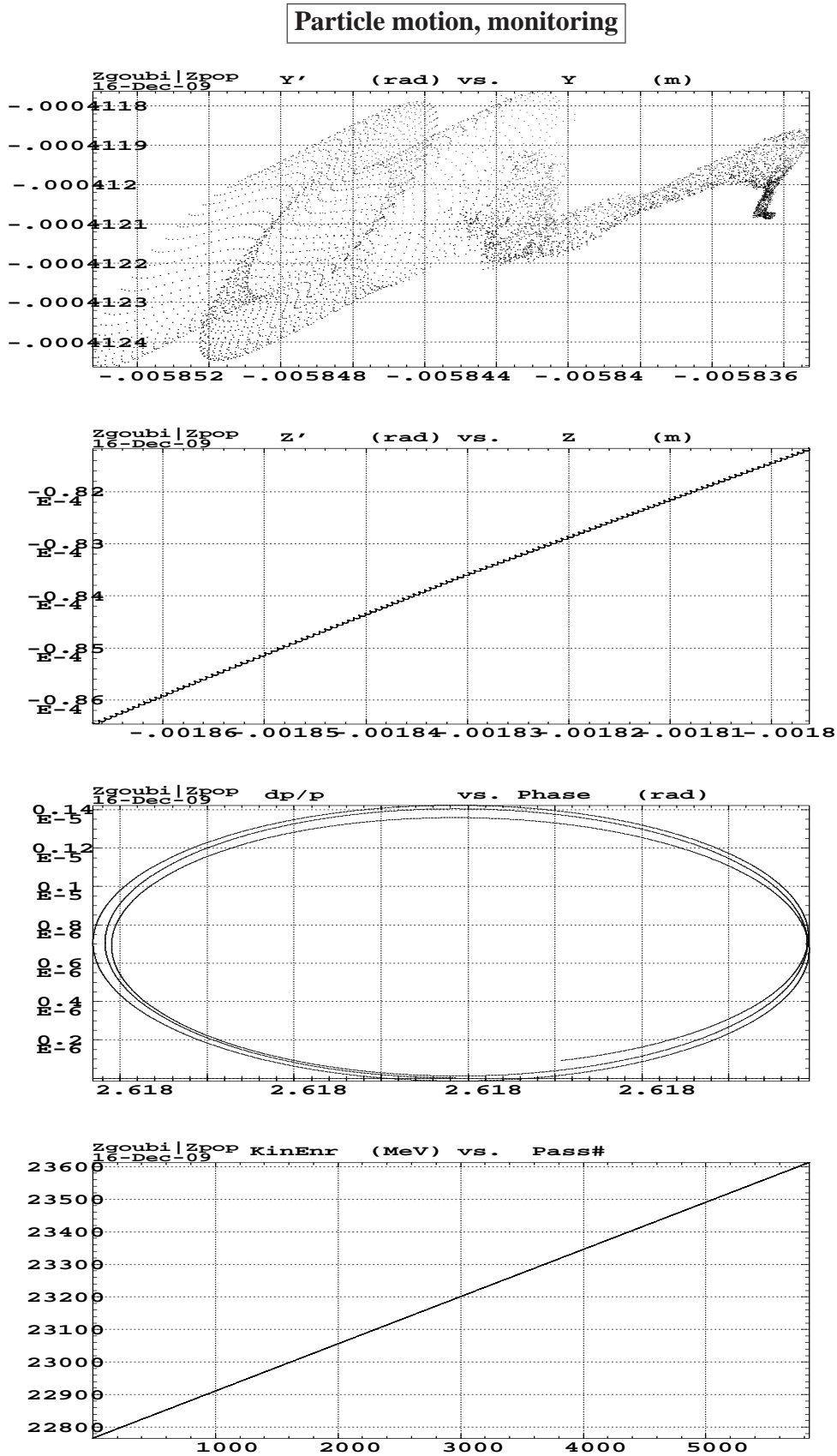


Figure 12: Particle motion. Top :  $x, x'$ , middle-up :  $z, z'$  ; middle-down : phase-dp/p ; these three graphs show good symplectic behavior. Bottom : kinetic energy versus turn number.



## 4.2 Non-zero horizontal emittance

We consider  $\beta\gamma\epsilon_x = 20\pi$  mm.mrad and starting  $\epsilon_y = 0$  (not for long : H-V coupling due to the snakes induces V motion) in this Section. Spin tracking results are displayed in Fig. 13. Particle dynamics behavior is monitored in Fig. 12.

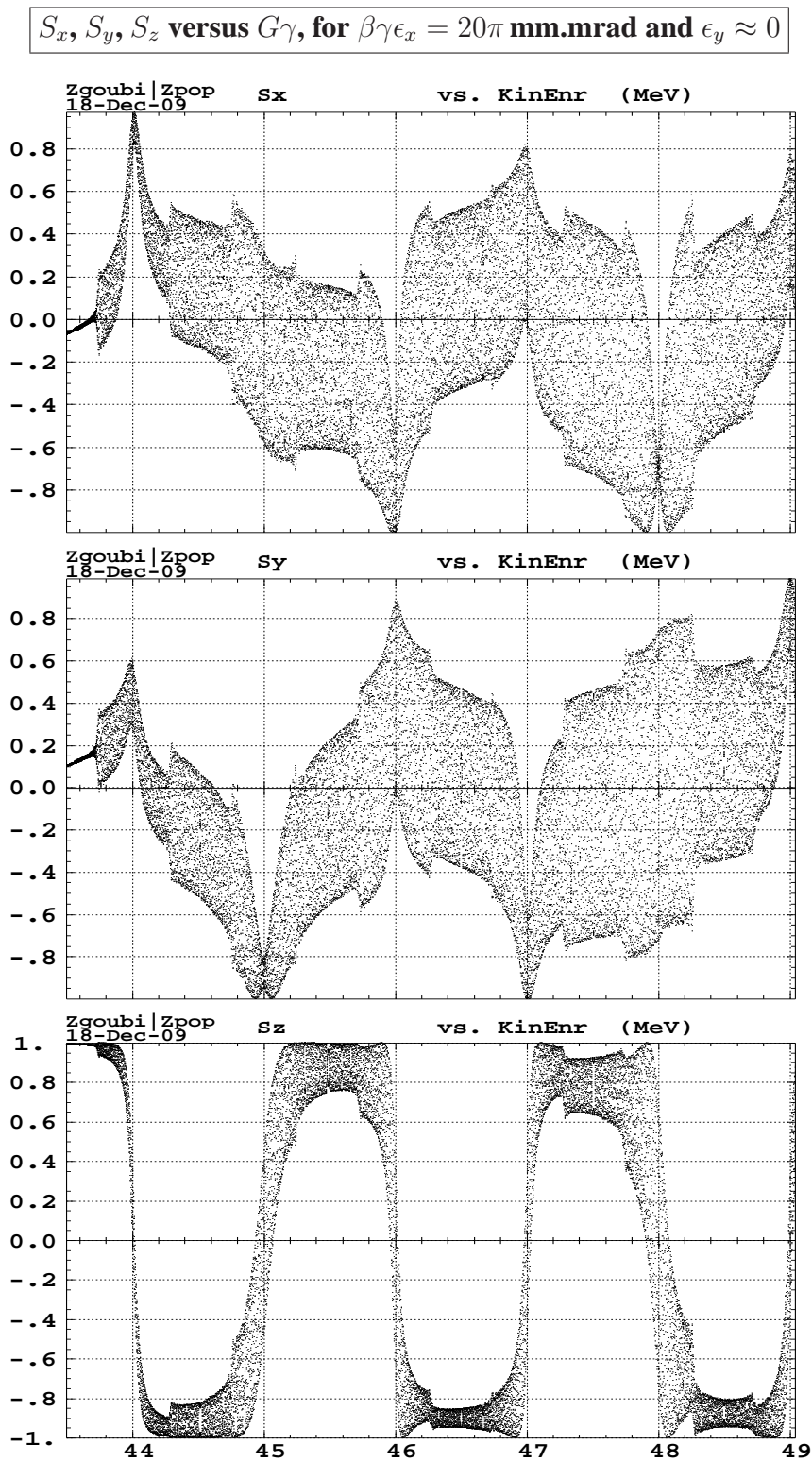


Figure 13: Spin motion experienced by the synchronous particle in presence of w- and c-snake, over  $G\gamma : 43.5 \rightarrow 49$ . The figure shows the spin components  $S_x$  (longitudinal),  $S_y$  (radial),  $S_z$  (vertical) (from top to bottom) as recorded in an arc.

The bottom graph clearly shows the effect of spin coupling resonances at  $G\gamma \pm Q_x = \text{integer}$ .



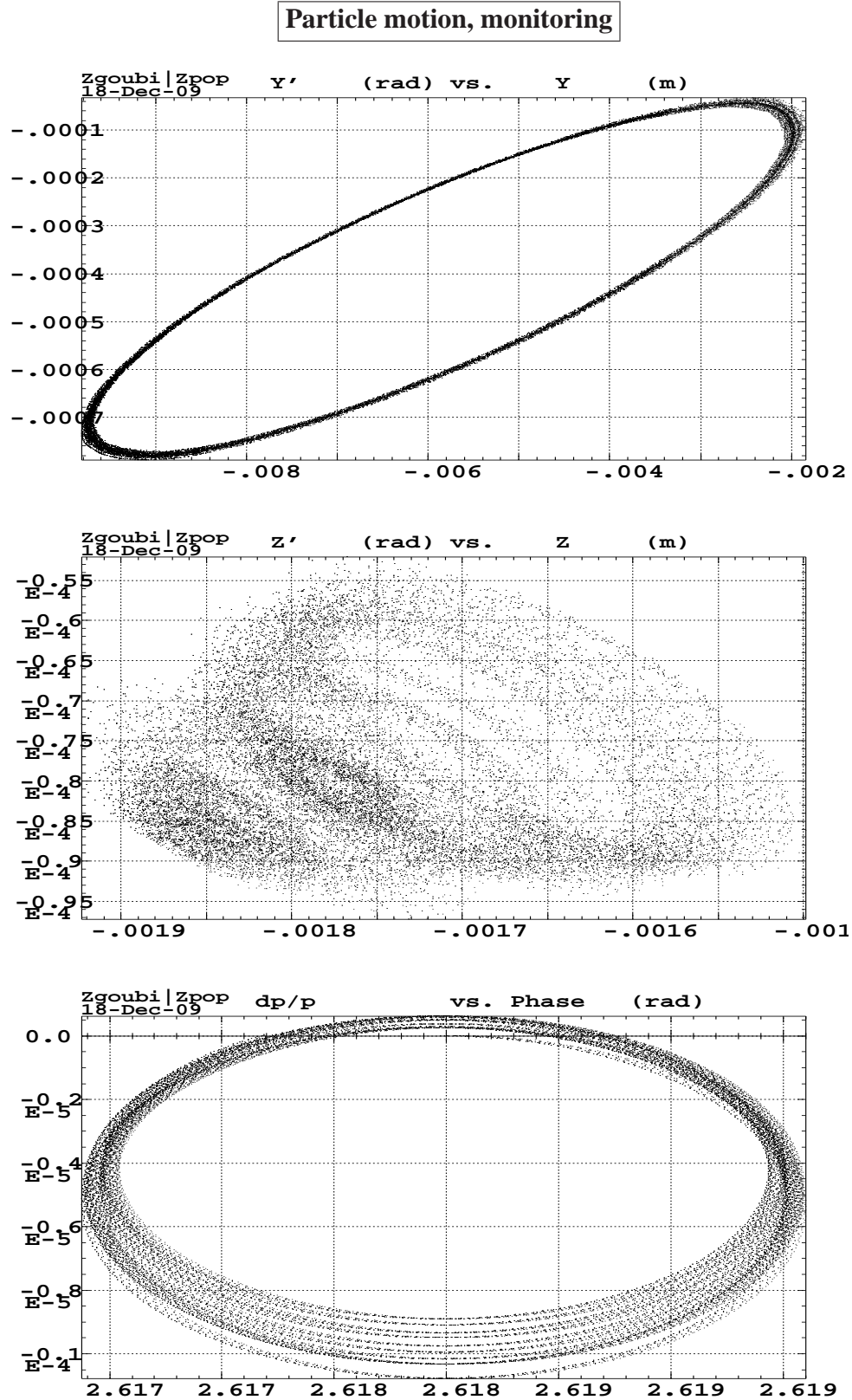


Figure 14: Particle motion, symplecticity. Top :  $x, x'$ , middle :  $z, z'$  ; bottom : phase-dp/p. H-V coupling (the snakes are the cause) induces V motion.

## 5 Spin tracking, $\gamma G = 43.5 \rightarrow 49$ , including Q-jump

Conditions are the same as in Section 4.2, in particular  $\beta\gamma\epsilon_x = 20\pi$  mm.mrad and starting  $\epsilon_y = 0$ .

A Q-jump scheme is added, causing  $\Delta\nu_x = 0.04$ , namely  $\nu_x : 8.73 \rightarrow 8.77$  (and also, since H and V controls are not fully separated,  $\nu_y : 8.9783 \rightarrow 0.9636$ ).

It uses two quads, QJUMI at I5A and QJUMJ at J5A. Their strengths satisfy  $K[\text{QJUMJ}] = K[\text{QJUMI}]$ , and approximately  $K[\text{QJUMI}] + K[\text{QJUMJ}] \approx \Delta\nu_x/\beta_x$ , with  $\beta_x \approx 25.65$  m at both quads.

Typical cycling of the two quads is shown in Fig. 15. Zgoubi allows free access to the starting point of the cycle ( $G\gamma = 43$  here), to the center point of the ramp in a period of the cycle (0.25 from the integer here), and to the length of the ramp ( $\pm 20$  turns around center point, here). The cycle is obtained using the 'SCALING' procedure, a new 'function generator' option, '-87', has been introduced for that - details concerning the input data (the content of zgoubi.dat) can be found on the next page and in App. B.5.

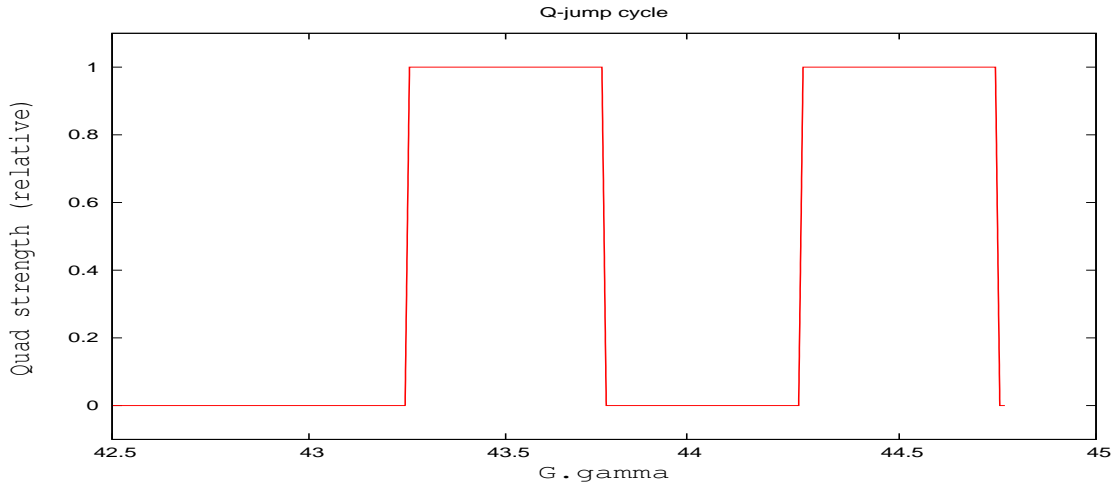


Figure 15: Q-jump cycle, causing  $\nu_x : 8.73 \rightarrow 8.77$ . The ramp up is centered at  $N + 0.25$ , the ramp down at  $N + 0.75$ , ramping in 40 turns.

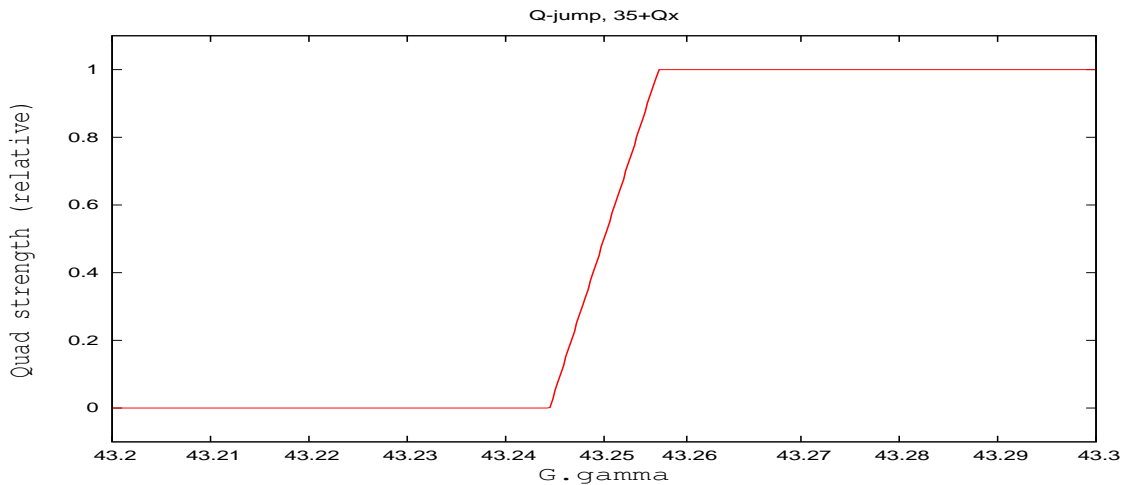


Figure 16: A zoom on the  $35 + \nu_x$  region. The ramp up here is centered at +0.25 from the integer.

**Input data to Zgoubi,** allowing a ramp in two jump quadrupoles QJUMI, QJUMJ.

This 'function generator' is based on the existing 'SCALING' keyword. An option ('-87') and three knobs (see below) have been added to allow control of the jump.

In the example below, Qjump cycling starts when  $G\gamma = 43$ , the ramps are centered at +0.25 (ramp up) and -0.75 (ramp down) from all subsequent integer  $G\gamma$ . The ramp length is 40 turns.

```
Data generated by searchCO
'OBJET' 1
75.8725752916200e3
2
1 1 CLOSED ORBIT COORDINATES :
-5.834246E-01 -4.120793E-01 -0.18669206 -8.64476501E-02 0.0E+00 1.00000000E+00 'o'
1
'FAISCEAU' 2
'SCALING' FUNCTION GENERATORS
1 3
MULTIPOL SBEN MAIN BENDS
-1
75.8725752916200 field factor
1
MULTIPOL QUAD QUADRUPOLES (UNUSED)
-1
75.8725752916200 field factor
1
MULTIPOL QJUMI QJUMJ JUMP QUADS
-87
75.8725752916200 field factor
43 0.25 40 43=starting G.gamma, N+/-0.25=center of ramp, 40 turns=length of ramp
'PARTICUL' 4
938.27203d0 1.602176487d-19 1.7928474d0 0. 0.
'MARKER' #Start 5
'MULTIPOL' SBEN A1BF 6
0 .Dip
200.6554 10.00 0.11712499 0.04844450 -0.00053604 0.0 0.0 0.0 0.0 0.0 0.0 0.0
0. 0. 10.00 4.0 0.800 0.00 0.00 0.00 0.00 0.0 0.0 0.0
4 .1455 2.2670 -1.6395 1.1558 0. 0. 0.
0. 0. 10.00 4.0 0.800 0.00 0.00 0.00 0.00 0.0 0.0 0.0
4 .1455 2.2670 -1.6395 1.1558 0. 0. 0.
0. 0. 0. 0. 0. 0. 0. 0. 0. 0. 0. 0.
#20|200|20 Dip A1BF
3 0. 0. -1.175115045000000E-002
.....
'MULTIPOL' QJUMI Betax, Alphax : 2.5743E+01 -1.9636E-01, Betax, Alphax : 8.9566 691
0 .Quad xco = -0.84698959, yco=-0.26546500
76.1927 10.00 0.0 0.01514 0.0 0.0 0.0 0.0 0.0 0.0 0.0 0.0
0. 0. 6.00 3.00 1.00 0.00 0.00 0.00 0.00 0.00 0.0 0.0 0.0
6 .1122 6.2671 -1.4982 3.5882 -2.1209 1.723
0. 0. 6.00 3.00 1.00 0.00 0.00 0.00 0.00 0.00 0.0 0.0 0.0
6 .1122 6.2671 -1.4982 3.5882 -2.1209 1.723
0. 0. 0. 0. 0. 0. 0. 0. 0. 0. 0. 0.
#30|76|30 Quad QJUMI
2 0. -0.8443957063 0.
.....
'MULTIPOL' QJUMJ 2.37xQJUMI Betax, Alphax: 2.5599E+01 -1.0912E-01, Betay, Alphay: 768
0 .Quad xco=-0.74307103, yco=-0.10033425 3.37*kl=4pi*dQ/betx=4pi*0.04/25.6=0.01963 bl(T)=Brho*(k
76.1927 10.00 0.0 0.01514 0.0 0.0 0.0 0.0 0.0 0.0 0.0 0.0
0. 0. 6.00 3.00 1.00 0.00 0.00 0.00 0.00 0.00 0.0 0.0 0.0
6 .1122 6.2671 -1.4982 3.5882 -2.1209 1.723
0. 0. 6.00 3.00 1.00 0.00 0.00 0.00 0.00 0.00 0.0 0.0 0.0
6 .1122 6.2671 -1.4982 3.5882 -2.1209 1.723
0. 0. 0. 0. 0. 0. 0. 0. 0. 0. 0. 0.
#30|76|30 Quad QJUMJ
2 0. -0.7406596043
.....
'CAVITE' 985
2 .1 .1 is to fill zgoubi.CAVITE.Out for plot using zpop/7/20
807.042748 12.
290.d3 2.617993877991494365 9cavitiesx32kV, phi_s=150deg
'MARKER' #End 986
'SPNRPT' 987
'FAISCEAU' 988
'REBELOTE' 989
19999 0.2 99
'END' 990
```

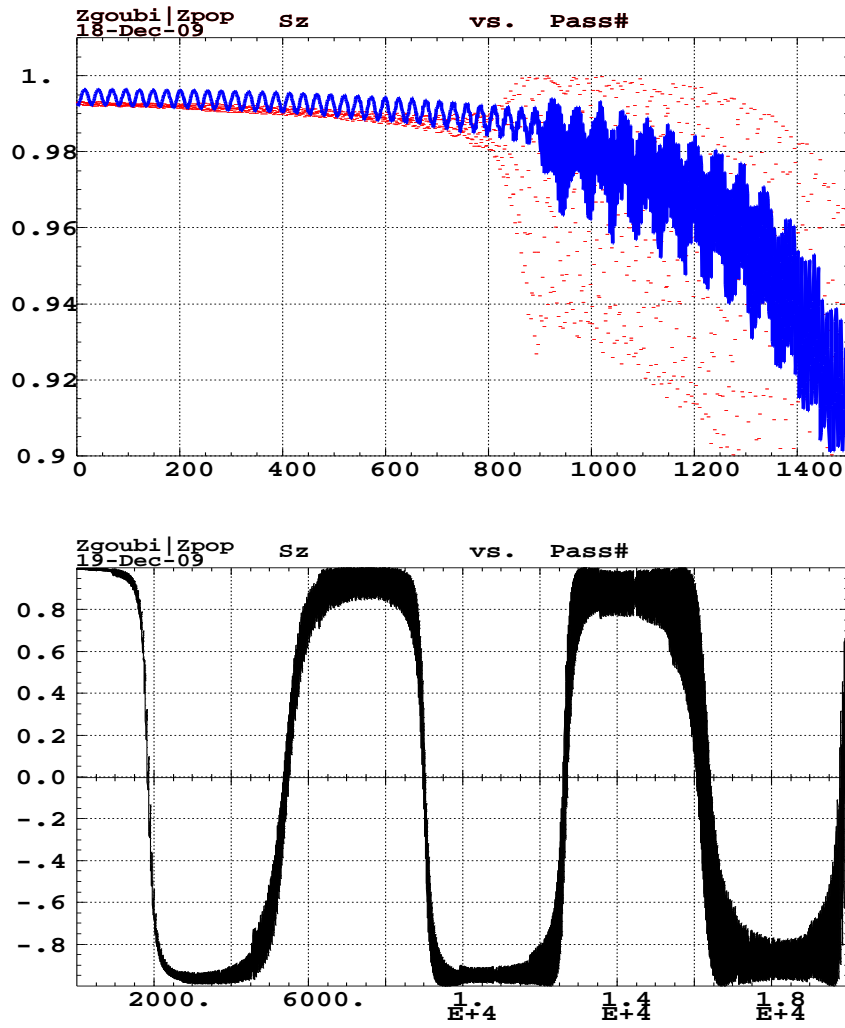


Figure 17: Vertical projection of  $\vec{S}$ .

Top : single particle, a zoom on the  $\nu_s = 35 + \nu_x$  region, with (blue dots) and without (red dots) Q-jump.

Bottom : single particle, acceleration from  $G\gamma = 43.5$  to  $G\gamma = 49$  in presence of Q-jump at all  $G\gamma \pm \nu_x$ .

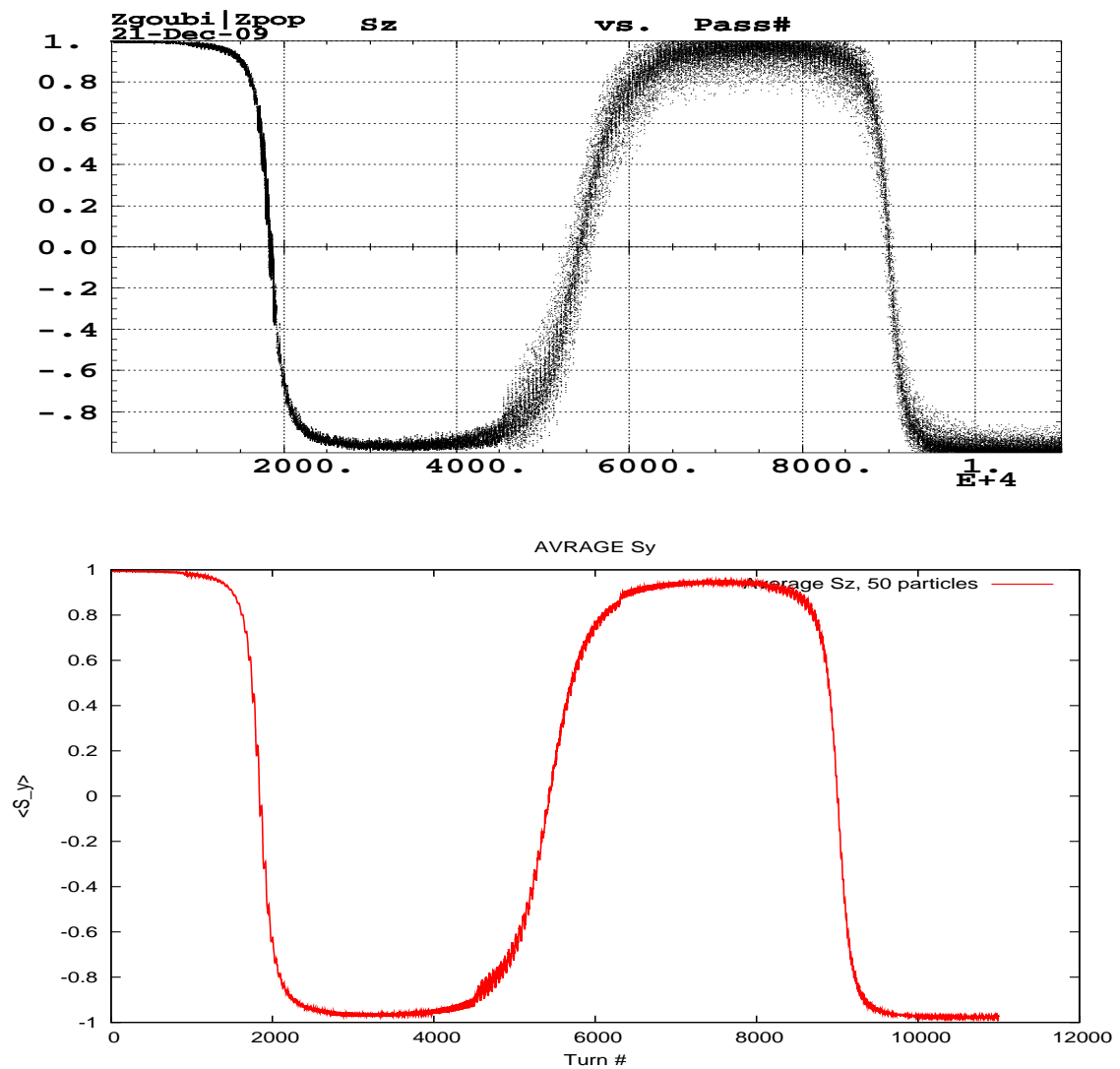


Figure 18: Vertical projection of  $\vec{S}$ , 50 particles taken at random in horizontal Gaussian distribution with  $\beta\gamma\epsilon = 2.5\pi$  mm.mrad.

Top : all 50 cases  $S_z(\text{turn}\#)$  are superimposed,

Bottom : average over the 50 particles, turn by turn.

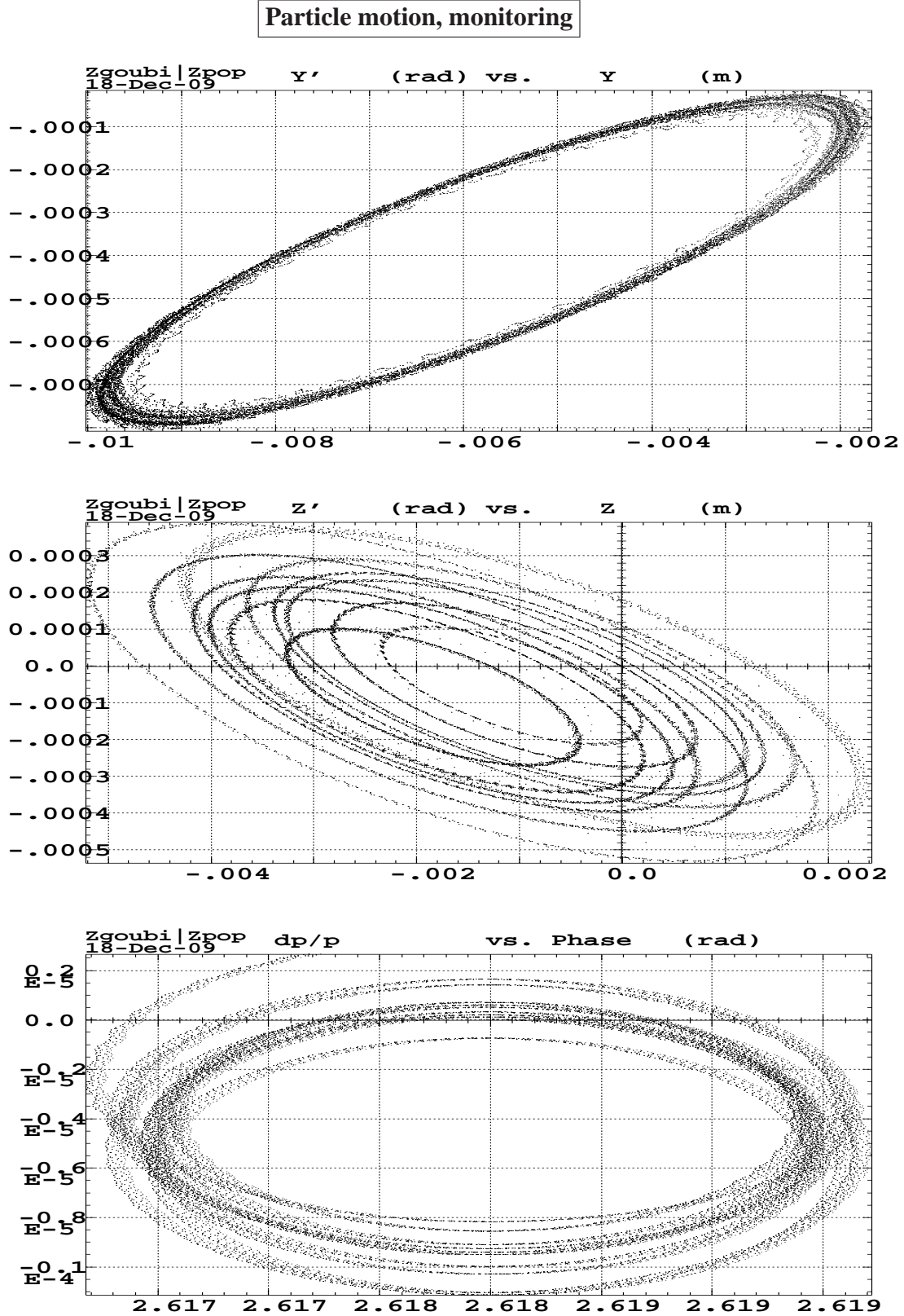


Figure 19: Particle motion, 20000 turns. Top :  $x, x'$ , middle :  $z, z'$  ; bottom : phase-dp/p. Note that, (i) the vertical emittance is not zero, this is due to coupling with  $(x, x')$  induced by the snakes ; (ii) the jump quadrupoles have not been vertically aligned, so that the jump causes a shift of the vertical ellipse in the  $(z, z')$  phase space.

### Improving beam dynamics

Non-zero horizontal closed orbit causes the quasi-zero vertical phase space portrait of Fig. 14 as obtained with jump quads off, to transform when jump quads are on into the vertical phase space portrait of Fig. 19 which shows both closed orbit effects (in particular the vertical closed orbit jumps during the on/off cycling of the quads) and induced vertical emittance. This behavior is due to H/V coupling induced by the snakes, correlated with so induced vertical closed orbit in the jump quads,

In the case of Fig. 19 the jump quadrupoles 'QJUMI' and 'QJUMJ' are centered onto their local horizontal closed orbit (by respective  $\Delta x = -0.8443$  cm and  $\Delta x = -0.7406$  cm, see data on page 16). Introducing further vertical centering of 'QJUMI' and 'QJUMJ' (respectively  $\Delta y = -0.8443$  cm and  $\Delta y = -0.7406$  cm, see page 22) does improve the vertical phase space portrait, see Fig. 21, namely, yielding quasi-zero phase portrait, closer to the jump quad free case shown in Fig. 14.

Matching H and V closed orbits to zero is performed using the 'FIT' procedure, see next page.

A new type of argument to the 'CHANGREF' procedure in Zgoubi (up to recently limited to X-, Y-shift and Z-rotation) has been developed for that purpose. It allows arbitrary sequence of up to 9 transforms, X-, Y-, Y-shift and X-, Y-, Z-rotation. Details on page 16.

Resulting spin behavior is displayed in Fig. 22. Clearly improvement is observed by comparison with Fig. 17, as to preservation of the polarization over  $G\gamma : 43.5 \rightarrow 49$ . Note that the spin vector is better matched at start as a consequence of zero-er closed orbit (initial particle as well as spin coordinates unchanged, same as in the case of Fig. 17).

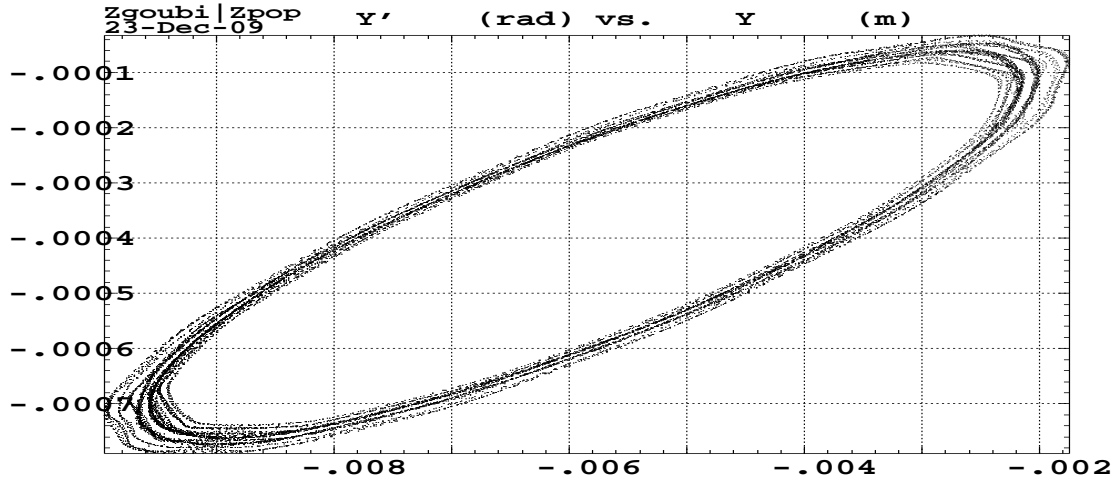


Figure 20: Particle motion, 16000 turns, improved H motion in presence of zero H and V closed orbits in jump quadrupoles. To be compared to Fig. 19-top with jump quads on and sole H centering, it can in particular be observed that the orbit jump upon jump quad on/off switching is better resolved.

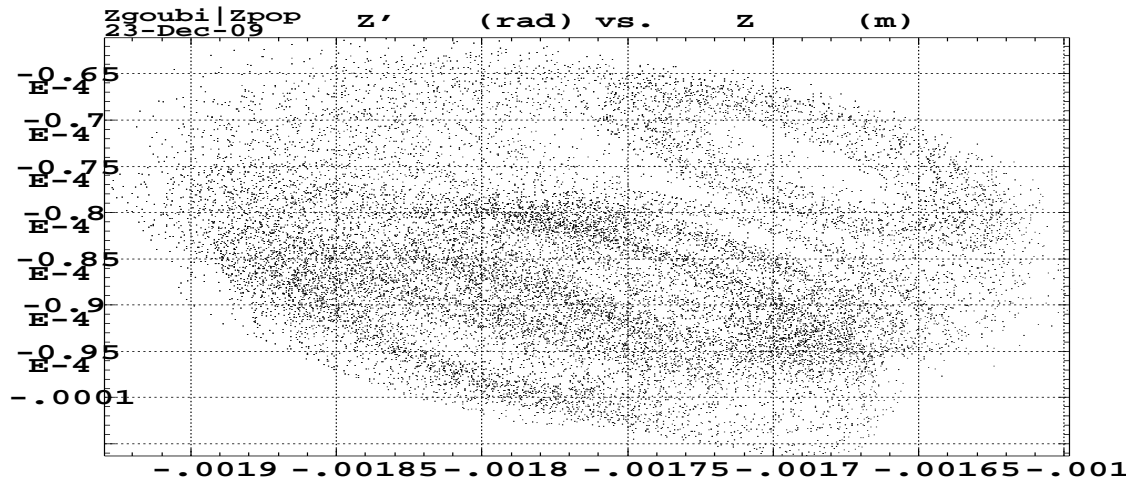


Figure 21: Particle motion, 16000 turns, quasi-zero vertical phase space portrait in presence of H&V centering of the jump quadrupoles on their local H and V closed orbits, to be compared to Fig. 19-middle with jump quads on and sole H centering, and to Fig. 14-middle with jump quads off.



Data generated by searchCO

```
'OBJET'
75.8725752916200e3
8
1 1 1
-5.834246E-03 -4.120793E-04 -0.18669206e-2 -8.64476501E-05 0.0E+00 1.00000000E+00
-1.475186 19.261771 .825e-6
0.830823 9.919738 0
0 1 0
'FAISCEAU' 2
'SCALING' 3
1 3
MULTIPOL SBEN
-1
75.8725752916200
1
MULTIPOL QUAD
-1
75.8725752916200
1
MULTIPOL QJUMI QJUMJ
-87
75.8725752916200
43 .235 40 starting Gg value, dN, #Turns/ramp
'PARTICUL' 4
938.27203d0 1.602176487d-19 1.7928474d0 0. 0.
'SPNTRK' 5
4.1
-6.8707152746E-02 0.1015767981 0.9924522556
'FAISTORE'
b_zgoubi.fai #End
1
'SPNSTORE'
b_zgoubi.spn #Start
1
'MARKER' #Start
'MULTIPOL' SBEN ALBF 8
0 .Dip
200.6554 10.00 0.11712499 0.04844450 -0.00053604 0.0 0.0 0.0 0.0 0.0 0.0 0.0 0.0
0. 0. 10.00 4.0 0.800 0.00 0.00 0.00 0.00 0.00 0. 0. 0. 0.
4 .1455 2.2670 -.6395 1.1558 0. 0. 0.
0. 0. 10.00 4.0 0.800 0.00 0.00 0.00 0.00 0.00 0. 0. 0.
4 .1455 2.2670 -.6395 1.1558 0. 0. 0.
0. 0. 0. 0. 0. 0. 0. 0. 0. 0.
#20|200|20 Dip ALBF
3 0. 0. -1.175115045000000E-002
.....
'CHANGREF' 690
YS -0.8422696264 ZS -0.2749666097
'MULTIPOL' QJUMI Betax, Alphax : 2.5743E+01 -1.9636E-01, Betax, Alphax : 8.9566E+00 -8.9363E-03
0 .Quad xco = -0.84698959, yco=-0.26546500
76.1927 10.00 0.0 0.01514 0.0 0.0 0.0 0.0 0.0 0.0 0.0 0.0 0.0
0. 0. 6.00 3.00 1.00 0.00 0.00 0.00 0.00 0.00 0. 0. 0. 0.
6 .1122 6.2671 -1.4982 3.5882 -2.1209 1.723
0. 0. 6.00 3.00 1.00 0.00 0.00 0.00 0.00 0.00 0. 0. 0. 0.
6 .1122 6.2671 -1.4982 3.5882 -2.1209 1.723
0. 0. 0. 0. 0. 0. 0. 0. 0. 0.
#30|76|30 Quad QJUMI
1 0. 0. 0.
'CHANGREF' 692
YS 0.8422696264 ZS 0.2749666097
.....
'CHANGREF' 767
YS -0.7387819677 ZS -7.6666666667E-02
'MULTIPOL' QJUMJ =QJUMI Betax, Alphax: 2.5599E+01 -1.0912E-01, Betax, Alphax: 8.1776E+00 3.2910E-02
0 .Quad xco=-0.74307103, yco=-0.10033425 3.7*kl=4pi*dQ/betx=4pi*0.04/25.6=0.01963 b1(T)=Brho*(kl/1*2.37/3.37)*a
76.1927 10.00 0.0 0.01514 0.0 0.0 0.0 0.0 0.0 0.0 0.0 0.0 0.0
0. 0. 6.00 3.00 1.00 0.00 0.00 0.00 0.00 0.00 0. 0. 0. 0.
6 .1122 6.2671 -1.4982 3.5882 -2.1209 1.723
0. 0. 6.00 3.00 1.00 0.00 0.00 0.00 0.00 0.00 0. 0. 0. 0.
6 .1122 6.2671 -1.4982 3.5882 -2.1209 1.723
0. 0. 0. 0. 0. 0. 0. 0. 0. 0.
#30|76|30 Quad QJUMJ
1 0. 0. 0.
'CHANGREF' 769
YS 0.7387819677 ZS 7.6666666667E-02
.....
.....
.....
Constraining zero H and V closed orbits in jump quads :
'FIT' 980
4 !!fit qjump position to center on closed orbit (i.e., so to get xco,zco=0 in qjumps)
690 1 -692.001 20.
690 2 -692.002 6.
767 1 -769.001 6.
767 2 -769.002 6.
4
3 1 2 690 0. 1. 0
3 1 4 690 0. 1. 0
3 1 2 767 0. 1. 0
3 1 4 767 0. 1. 0
'END' 981
```

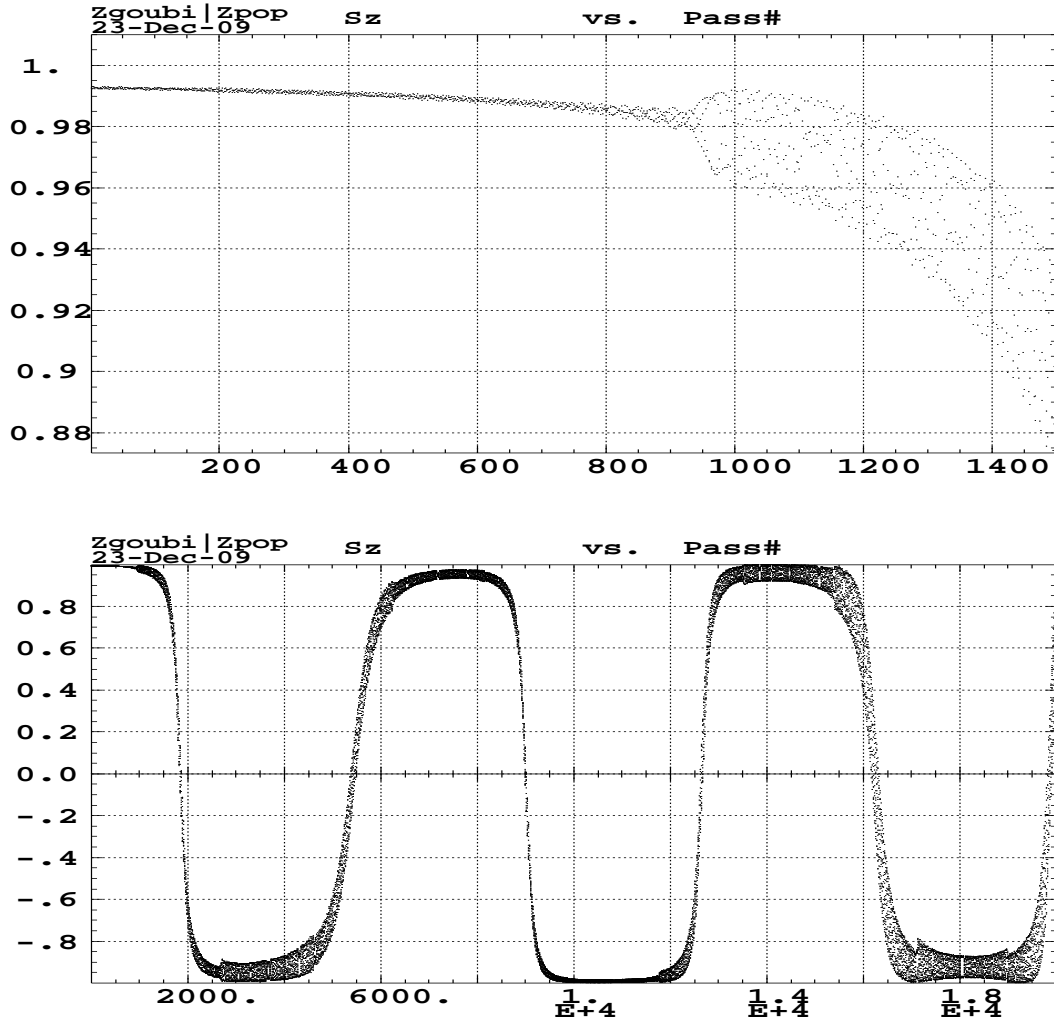


Figure 22: Vertical projection of  $\vec{S}$ , single particle, in presence of H & V closed orbit in jump quads. To be compared to Fig. 17.  
 Top : a zoom on the  $\nu_s = 35 + \nu_x$  region.  
 Bottom : acceleration, from  $G\gamma = 43.5$  to  $G\gamma = 49$ .

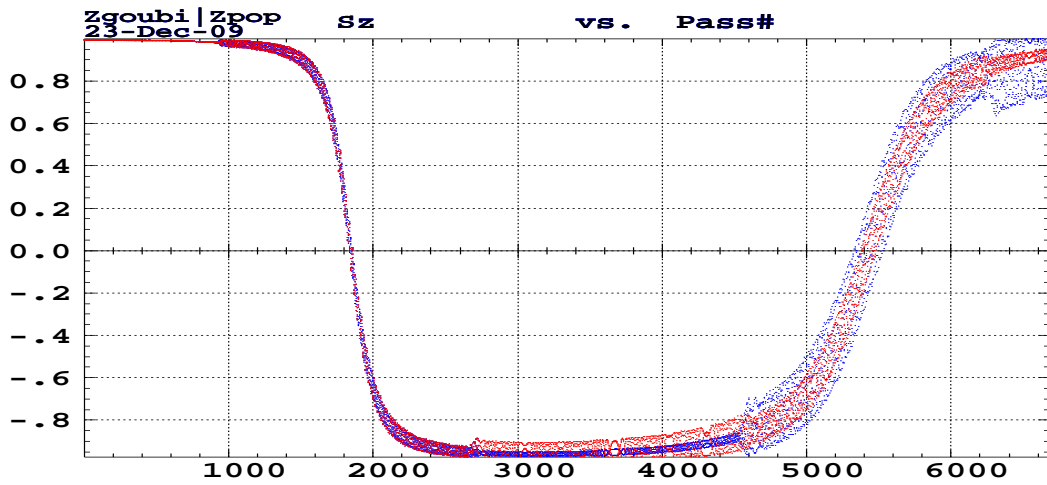


Figure 23: Vertical projection of  $\vec{S}$ , two particles. Conditions differ by the value of 'dN' in the argument of 'SCALING', namely,  $dN=0.237$  (red) and  $dN=0.244$  (blue).

## APPENDIX

## A MAD files

Excerpts of MAD files are reproduced, for reference.

## A.1 Command file

```

Title, "AGS+cv43+755 snakes. 2quad sol. AUL matrices"
!-----Physical constants-----
CONV: constant=0.0254 !meter per inch
E0: constant= 0.938272310 !proton mass [GeV]
C: constant= 2.99792458e8 !speed of light [m/sec]
!-----Machine parameters-----
RHO: constant=85.378 !AGS curv. radius [m]
DIPL: constant=999 !AGS dipole calibration [T/A]
!-----
!
! gamma:=24.264 !!!24.385706
! call 'gamma.ins'
!-----
setopts, -echo
EE := E0*GAMMA ; Ek := EE - E0 ; PC := sqrt(EE*EE - E0*E0)
BRHO := 1.e9*PC/C ; BETA := sqrt(1-1/((1+Ek/E0)*(1+Ek/E0))) ;
B := BRHO/RHO
value GAMMA ; value PC ; value EE ; value Ek ; value BETA ; value BRHO ;
value B

beam, particle=proton, pc=PC
!PCINJ:=1.143 !this is the equivalent with gold beam, if betagamma=0.48
PCINJ:=2.303 !this is injection momentum
BDOT := 0. ; DK2 := 0.04244*BDOT*PCINJ/PC !where is this from?
call 'lattice/ags4.lat' !lattice file
!call 'kickstrength.ins' !kickers strength
!!
!! Snakes represented by a matrix. 3 m long. AUL July 03
SNAKE: marker ; DSNK: drift, l=0.023839 !
!
! call 'CSNK_B2.0_NoSol.Tmat/SY_CSNK_B2.0_243.mat' !!!!!1243 means 23.4=gamma
! call 'CSNK_B2.5+0.75sol.Tmat/CSNK_B2.5+0.75sol_49.mat'
CSNKL: line=(DSNK,CSNK,SNAKE,DSNK) !cv43 cold snake line !
! CSNKL: line=(DSNK,DRFMAT,SNAKE,DSNK) !cv43 cold snake line !
!
! call 'WSNK_B1.53.Tmat/WSNK_B1.53_243.mat'
WSNKL: line=(DSNK,WSNK,SNAKE,DSNK) !t55 warm snake line !
! WSNKL: line=(DSNK,DRFMAT,SNAKE,DSNK) !t55 warm snake line !

setopts, echo
!!-----
!! Quad scales
BRHOO := 7.17113418 ! at gamma=2.5
BRHOScale:= (BRHOO/BRHO)*(BRHOO/BRHO)
!
!call 'Csnake_field.ins'
!BCSNAKE := 2.5
!Cscale:= (BCSNAKE/3.123)*(BCSNAKE/3.123)
!
!call 'Wsnake_field.ins'
!BWSNAKE := 1.53
!Wscale:= (BWSNAKE/3.123)*(BWSNAKE/3.123)

!Bscale := (1.53/2.5)*(1.53/2.5)
Bscale := (1.53/2.0)*(1.53/2.0)
!!-----
!! Courant quadrupoles
!COLD SNAKE, WARM SNAKE
!KCA17:=-0.1012; KCA19:=-0.21513; KCB1:=-0.26535; KCB3:=-0.15387
!KCE17:=-0.17495;KCE19:=0.21857;KCF1:=-0.21857;KCF3:=0.

!!!!comment-----for 15% Cold snake -----
!KCA17C:=-0.232498891301*BRHOScale !-0.096498967516
!KCA19:=-0.116067942892*BRHOScale !-0.21 !-0.21192166075
!KCB1 :=-0.256023389862*BRHOScale !-0.21 !KCA19 !-0.288662622487
!KCB3 :=-0.111548158531*BRHOScale !-0.152715283932
!
!KCE17C:=-0.105710632359*BRHOScale !-0.147949275317
!KCE19:= 0.23558686779491*BRHOScale !0.072 ! 0.0747633511
!KCF1 :=-0.23552239053742*BRHOScale !-KCE19 !-0.069533016847
!KCF3 := 0.098109749898*BRHOScale !-0.084075610041
!!!!endcomment-----for 15% Cold snake -----

!!!!comment-----for 10% Cold snake -----
KCA17C:=-0.232498891301*0.8*BRHOScale !-0.096498967516
KCA19:=-0.116067942892*0.8*BRHOScale !-0.21 !-0.21192166075
KCB1 :=-0.256023389862*0.8*BRHOScale !-0.21 !KCA19 !-0.288662622487
KCB3 :=-0.111548158531*0.8*BRHOScale !-0.152715283932
!
KCE17C:=-0.105710632359*0.8*BRHOScale !-0.147949275317
KCE19:= 0.23558686779491*0.8*BRHOScale !0.072 ! 0.0747633511
KCF1 :=-0.23552239053742*0.8*BRHOScale !-KCE19 !-0.069533016847
KCF3 := 0.098109749898*0.8*BRHOScale !-0.084075610041
!!!!endcomment-----for 10% Cold snake -----
!!-----

```

```

!! Tune Quad currents [A]
!XQH := 13.08 ; XQV := -23.408
!KQH := 0.0 ; KQV := 0.0
!KQJM := 0.01
!KQH := 0.179079846975E-01; KQV := -0.249486131375E-02 ! Gg 4.5
!KQJM := 0.0129331838272
!KQJM := 0.012701886853
KQH := 0.166268687200E-01; KQV := -0.380045229870E-01 ! Gg 43.5
KQJM := 0.0142600853986
LENQC := 0.35 ; LDSQC = (LDSQ - LENQC)/2.
D2SC: drift, l=(LD2S - LENQC)/2. ; DSQC: drift, l=LDSQC
KCA17:= KCA17C + KQH
QCA17: quad, l=LENQ, k1=KCA17
QCA19: quad, l=LENQC, k1=KCA19
QCB1 : quad, l=LENQC, k1=KCB1
QCB3 : quad, l=LENQ, k1=KCB3
DSQH: drift, l=LDSQ+LENQ
DSQV: drift, l=LD5L/2-LENQC
KCE17:= KCE17C + KQH
QCE17: quad, l=LENQ, k1=KCE17
QCE19: quad, l=LENQC, k1=KCE19
QCF1 : quad, l=LENQC, k1=KCF1
QCF3 : quad, l=LENQ, k1=KCF3

D2SX: drift, L=(23.99664*CONV - LQB1)/2 !=0.154757
!
-----
use, AGS_CW
!
!-----Match-----
cell
! vary, XQH, step=0.1, lower=-2000., upper=2000.
! vary, XQV, step=0.1, lower=-2000., upper=2000.
  vary, KQH, lower=-0.05, upper=0.04, step=0.00001
  vary, KQV, lower=-0.04, upper=0.01, step=0.00001
  constraint, range=#E, MUX=8.72, MUY=8.98
  lmdif, calls=2000, tolerance=1.0e-9
endmatch

! call file='ags.tune'
!-----
!MATCH
!comment
!cell
!vary, XQH, lower=-700, upper=700, step=0.001
!vary, XQV, lower=-700, upper=700, step=0.001
!vary, KQH, lower=-0.05, upper=0.04, step=0.00001
!vary, KQV, lower=-0.05, upper=0.04, step=0.00001
!vary, KQJM, lower=-0.1, upper=0.1, step=0.00001

!call "match.ins"
! constraint, #e, mux= 8.719
! constraint, #e, mux= 8.619
! constraint, #e, muy= 8.969

!simplex, calls=60000, tolerance=1e-9
!endmatch
!endcomment
!
-----

print, #E

select, flag=FIRST, range=#S/#E
  survey, tape='ags.survey'
twiss, tunes='Q.psh', tape='ags.twiss', deltap=0.
archive, table='Q.psh'

push, KQH, KQV, KQJM, Qx, Qy
endpush, save='quad.psh'

push, gamma, KCA17, KCA19, KCB1, KCB3, KCE17, KCE19, KCF1, KCF3, KQH, KQV
endpush, save='quadK1.psh'
push, gamma, K1AD, K1AF, K1BD, K1BF, K1CD, K1CF
endpush, save='dipK1.psh'

stop

```

## A.2 “dipole1” file

### Description of the superperiods in MAD8 using 'SBEND'

```

LENA = 2.3876 !94*CONV !length in meters
LENB = 2.0066 !79*CONV
LENC = 2.3876 !94*CONV

ANGA = 0.0279650307 !angle in radians
ANGB = 0.0235023009
ANGC = 0.0279650307

!Dipole Names
AD: sbend, l=LENA, angle=ANGA, k1=K1AD, k2=K2AD, e1=ANGA/2., e2=ANGA/2.
AF: sbend, l=LENA, angle=ANGA, k1=K1AF, k2=K2AF, e1=ANGA/2., e2=ANGA/2.
BD: sbend, l=LENB, angle=ANGB, k1=K1BD, k2=K2BD, e1=ANGB/2., e2=ANGB/2.
BF: sbend, l=LENB, angle=ANGB, k1=K1BF, k2=K2BF, e1=ANGB/2., e2=ANGB/2.
CD: sbend, l=LENC, angle=ANGC, k1=K1CD, k2=K2CD, e1=ANGC/2., e2=ANGC/2.
CF: sbend, l=LENC, angle=ANGC, k1=K1CF, k2=K2CF, e1=ANGC/2., e2=ANGC/2.

```

```

A1BF: BF ; A2BF: BF ; A3CD: CD ; A4CD: CD ; A5AF: AF
A6AF: AF ; A7CD: CD ; A8CD: CD ; A9BF: BF ; A10BF: BF
A11BD: BD ; A12BD: BD ; A13CF: CF ; A14CF: CF ; A15AD: AD
A16AD: AD ; A17CF: CF ; A18CF: CF ; A19BD: BD ; A20BD: BD

B1BF: BF ; B2BF: BF ; B3CD: CD ; B4CD: CD ; B5AF: AF
B6AF: AF ; B7CD: CD ; B8CD: CD ; B9BF: BF ; B10BF: BF
B11BD: BD ; B12BD: BD ; B13CF: CF ; B14CF: CF ; B15AD: AD
B16AD: AD ; B17CF: CF ; B18CF: CF ; B19BD: BD ; B20BD: BD

C1BF: BF ; C2BF: BF ; C3CD: CD ; C4CD: CD ; C5AF: AF
C6AF: AF ; C7CD: CD ; C8CD: CD ; C9BF: BF ; C10BF: BF
C11BD: BD ; C12BD: BD ; C13CF: CF ; C14CF: CF ; C15AD: AD
C16AD: AD ; C17CF: CF ; C18CF: CF ; C19BD: BD ; C20BD: BD

D1BF: BF ; D2BF: BF ; D3CD: CD ; D4CD: CD ; D5AF: AF
D6AF: AF ; D7CD: CD ; D8CD: CD ; D9BF: BF ; D10BF: BF
D11BD: BD ; D12BD: BD ; D13CF: CF ; D14CF: CF ; D15AD: AD
D16AD: AD ; D17CF: CF ; D18CF: CF ; D19BD: BD ; D20BD: BD

E1BF: BF ; E2BF: BF ; E3CD: CD ; E4CD: CD ; E5AF: AF
E6AF: AF ; E7CD: CD ; E8CD: CD ; E9BF: BF ; E10BF: BF
E11BD: BD ; E12BD: BD ; E13CF: CF ; E14CF: CF ; E15AD: AD
E16AD: AD ; E17CF: CF ; E18CF: CF ; E19BD: BD ; E20BD: BD

F1BF: BF ; F2BF: BF ; F3CD: CD ; F4CD: CD ; F5AF: AF
F6AF: AF ; F7CD: CD ; F8CD: CD ; F9BF: BF ; F10BF: BF
F11BD: BD ; F12BD: BD ; F13CF: CF ; F14CF: CF ; F15AD: AD
F16AD: AD ; F17CF: CF ; F18CF: CF ; F19BD: BD ; F20BD: BD

G1BF: BF ; G2BF: BF ; G3CD: CD ; G4CD: CD ; G5AF: AF
G6AF: AF ; G7CD: CD ; G8CD: CD ; G9BF: BF ; G10BF: BF
G11BD: BD ; G12BD: BD ; G13CF: CF ; G14CF: CF ; G15AD: AD
G16AD: AD ; G17CF: CF ; G18CF: CF ; G19BD: BD ; G20BD: BD

H1BF: BF ; H2BF: BF ; H3CD: CD ; H4CD: CD ; H5AF: AF
H6AF: AF ; H7CD: CD ; H8CD: CD ; H9BF: BF ; H10BF: BF
H11BD: BD ; H12BD: BD ; H13CF: CF ; H14CF: CF ; H15AD: AD
H16AD: AD ; H17CF: CF ; H18CF: CF ; H19BD: BD ; H20BD: BD

I1BF: BF ; I2BF: BF ; I3CD: CD ; I4CD: CD ; I5AF: AF
I6AF: AF ; I7CD: CD ; I8CD: CD ; I9BF: BF ; I10BF: BF
I11BD: BD ; I12BD: BD ; I13CF: CF ; I14CF: CF ; I15AD: AD
I16AD: AD ; I17CF: CF ; I18CF: CF ; I19BD: BD ; I20BD: BD

J1BF: BF ; J2BF: BF ; J3CD: CD ; J4CD: CD ; J5AF: AF
J6AF: AF ; J7CD: CD ; J8CD: CD ; J9BF: BF ; J10BF: BF
J11BD: BD ; J12BD: BD ; J13CF: CF ; J14CF: CF ; J15AD: AD
J16AD: AD ; J17CF: CF ; J18CF: CF ; J19BD: BD ; J20BD: BD

!!special nomenclature required here due to overlaps
!!also appears in definiton of K superperiod

K1PBF: BF ; K2PBF: BF ; K3CD: CD ; K4CD: CD ; K5AF: AF
K6AF: AF ; K7CD: CD ; K8CD: CD ; K9BF: BF ; K10BF: BF
K11BD: BD ; K12BD: BD ; K13CF: CF ; K14CF: CF ; K15AD: AD
K16AD: AD ; K17CF: CF ; K18CF: CF ; K19BD: BD ; K20BD: BD

L1BF: BF ; L2BF: BF ; L3CD: CD ; L4CD: CD ; L5AF: AF
L6AF: AF ; L7CD: CD ; L8CD: CD ; L9BF: BF ; L10BF: BF
L11BD: BD ; L12BD: BD ; L13CF: CF ; L14CF: CF ; L15AD: AD
L16AD: AD ; L17CF: CF ; L18CF: CF ; L19BD: BD ; L20BD: BD

return
    
```

### A.3 “print” file

```

-----
LAGS+cv43+755 snakes. 2quad sol. AUL matrices                "MAD" Version: 8.23/08   Run: 01/10/09 12.36.37
Linear lattice functions.      TWISS                          line: AGS_CW           range: #S/#E
Delta(p)/p:      0.000000      symm: F                  super:      1
-----
ELEMENT SEQUENCE      I      H O R I Z O N T A L      I      V E R T I C A L
pos. element occ.      dist I  betax  alfax  mux  x(co)  px(co)  Dx  Dpx  I  betay  alfay  muy  y(co)  py(co)  Dy  Dpy
no.  name  no.  [m]  I  [m]  [1]  [2pi] [mm]  [.001] [m]  [1]  I  [m]  [1]  [2pi] [mm]  [.001] [m]  [1]
-----
begin AGS_CW      1      0.000  19.455 -1.537  0.000  0.0000  0.000  1.990  0.120  9.682  0.808  0.000  0.0000  0.000 -0.011  0.000
end   AGS_CW      1      807.076  19.455 -1.537  8.720  0.0000  0.000  1.990  0.120  9.682  0.808  8.980  0.0000  0.000 -0.011  0.000
-----
total length =      807.075652      Qx      =      8.720000      Qy      =      8.980000
delta(s)      =      0.000000 mm      Qx'     =      -22.470306      Qy'     =      2.698546
alfa          =      0.138967E-01      betax(max) =      25.738300      betay(max) =      27.478694
gamma(tr)     =      8.482905      Dx(max)   =      2.423274      Dy(max)   =      0.024185
                                         Dx(r.m.s.) =      1.811437      Dy(r.m.s.) =      0.013532
                                         xco(max)   =      0.000000      yco(max)   =      0.000000
                                         xco(r.m.s.) =      0.000000      yco(r.m.s.) =      0.000000
-----
    
```

## B Zgoubi data file specimen

### B.1 1-turn first order mapping, input file

Typical zgoubi.dat file including snakes and appropriate commands for MATRIX calculation including chromaticities, etc.

```
Data generated by searchCO
'OBJET'
75.8725752916200e3
5.03
.1 .001 .001 .001 0. .001
-7.847E-01 -5.374E-01 -1.638E-01 -6.812E-02 0E+00 9.990E-01 'o'
-5.834E-01 -4.120E-01 -1.862E-01 -8.664E-02 0E+00 1.000E+00 'o'
-3.809E-01 -2.865E-01 -2.184E-01 -1.160E-01 0E+00 1.001E+00 'o'
'FAISCEAU'
'SCALING'
1 2
MULTIPOL SBEN
-1
75.8725752916200
1
MULTIPOL QUAD
-1
75.8725752916200
1
'PARTICUL'
938.27203d0 1.602176487d-19 1.7928474d0 0. 0.
'PICKUPS'
1
#End
'FAISTORE'
b_zgoubi.fai
1
'MARKER' #Start
'MARKER' Begin
'MULTIPOL' SBEN ALBF
0 .Dip
200.6554 10. 0.11712499 0.0484445 -0.00053604 0 0 0 0 0 0 0
0. 0. 10.00 4.0 0.800 0.00 0.00 0.00 0.00 0.00 0.00 0.00
4 .1455 2.2670 -.6395 1.1558 0. 0. 0.
0. 0. 10.00 4.0 0.800 0.00 0.00 0.00 0.00 0.00 0.00 0.00
4 .1455 2.2670 -.6395 1.1558 0. 0. 0.
0 0 0 0 0 0 0 0 0. 0.
#20|200|20 Dip ALBF
3 0.00 0.000 -1.175115045000000E-002
'DRIFT' DRIF D2S
60.9515
.....
'DRIFT' DRIF DSNK
2.3839
'MARKER' MATR CSNK
'DRIFT' DRIF MATR CSNK
10.0000
'MAP2D'
0 0
.7e-3 100. 100. 100.
HEADER_4 csnake
281 29
ref+sole.map2d
0 0 0 0
2
.1
2 0. .15 0. 0.
'DRIFT'
10.0000
.....
'DRIFT' DRIF DSNK
2.3839
'MARKER' MATR WSNK
'DRIFT' DRIF MATR WSNK
-50.
'MARKER' MATR WSNK
'MAP2D'
0 0
1.e1 100. 100. 100.
HEADER_4 wsnoise
801 29
table55.map2d
0 0 0 0
2
.1
2 0. .15 0. 0.
'DRIFT' DRIF MATR WSNK
-50.
'MARKER' MARK SNAKE
'DRIFT' DRIF DSNK
2.3839
.....
'MULTIPOL' HKIC SML20
0 .kicker
0.2413E+03 10.00 0.0 0. 0.0 0.0 0.0 0.0 0.0 0.0 0.0 0.0 0.0
.0 .0 1.00 0.00 0.00 0.00 0.00 0.0 0. 0. 0. 0.
```

```
4 .1455 2.2670 -.6395 1.1558 0. 0. 0.
.0 .0 1.00 0.00 0.00 0.00 0.00 0.00 0. 0. 0. 0.
4 .1455 2.2670 -.6395 1.1558 0. 0. 0.
0.000000000 0 0 0 0 0 0 0. 0.
#20|20|20 Kick
1 0. 0. 0.
'DRIFT' DRIF DSG10
31.7339
'MARKER' #End
'FAISCEAU'
'MATRIX'
1 11
'FAISCEAU'
'END'
```

### B.2 Acceleration, using "CAVITE"

```
'CAVITE'
2.1 .1 is to fill zgoubi.CAVITE.Out for plot using zpop/7/20
807.042748 12. 0435
290.d3 2.617993877991494365 9cavitiesx32kV, phi_s=30deg
'MARKER' #End
```

### B.3 zgoubi.dat for w- and c-snake

Snake files, 3 meter extent, using 3D field maps.  
Warm snake :

```
WSNK
'OBJET'
77.64321e3
2
1 1
.0 0. . 0. 0. 1. 'o'
1
'PARTICUL'
938.27203d0 1.602176487d-19 1.7928474d0 0. 0.
'SPNTRK'
3
'TOSCA'
0 1
1.e1 100. 100. 100.
HEADER_4 csnake
801 29 29 12.1
table55.tab
0 0 0 0
2
.1
2 -0.15 0. 0. 0.
'FAISCEAU'
'END'
```

Cold snake :

```
CSNK
'OBJET'
77.64321e3
2
1 1
-.15 0. 0. 0. 0. 1. 'o'
1
'PARTICUL'
938.27203d0 1.602176487d-19 1.7928474d0 0. 0.
'SPNTRK'
3
'TOSCA'
0 1
1.e-3 100. 100. 100.
HEADER_4 csnake
281 29 29 12.1
ref+sole.tab
0 0 0 0
2
1
2 0. 0. 0. 0.
'FAISCEAU'
'END'
```

Snake data, 3 meter extent, using mid-plane 2D field maps.

See App. B.1.

## B.4 Spin $\vec{n}$ -vector

Typical zgoubi.dat data for spin- $\vec{n}$  vector finding using the 'FIT' procedure.

```
Data generated by searchCO
'OBJET'
75.8725752916200e3
2
 1 1
-5.834E-01 -4.120E-01 -0.1866 -8.644E-02 0.0E+00 1.E+00 'o'
1 1 1 1 1
'FAISCEAU'
'SCALING'
1 2
MULTIPOL SBEN
-1
75.8725752916200
1
MULTIPOL QUAD
-1
75.8725752916200
1
'PARTICUL'
938.27203d0 1.602176487d-19 1.7928474d0 0. 0.
'SPNTRK'
4.1
-6.8608394896E-02 0.1001299394 0.9926061069
'MARKER' Begin
'MULTIPOL' SBEN ALBF
0 .Dip
200.6554 10.00 0.1171 0.0484 -0.00053604 0 0 0 0 0 0 0
0. 0. 10.00 4.0 0.800 0.00 0.00 0.00 0.00 0. 0. 0. 0.
.....
'FIT' 3
5 10 0 2 Sx_0 variable
5 11 0 2 Sy_0
5 12 0 1 Sz_0
4
10.1 1 1 980 0. .3 0 Sx_final = Sx_0 constraint
10.1 1 2 980 0. .3 0 Sy_final = Sy_0
10.1 1 3 980 0. 1. 0 Sz_final = Sz_0
10 1 4 980 1. 2. 0 |S|=1
'END'
```

## B.5 Q-jump

Typical zgoubi.dat data for Q-jump simulation.

```
Data generated by searchCO
'OBJET'
75.8725752916200e3
2
 1 1
-5.834E-01 -4.120E-01 -0.18669 -8.6447E-02 0. 1.00E+00 'o'
1 1 1 1 1
'FAISCEAU'
'SCALING'
1 3
MULTIPOL SBEN
-1
75.8725752916200
1
MULTIPOL QUAD
-1
75.8725752916200
1
MULTIPOL QJUMI QJUMJ
-87
75.8725752916200
44 .25 40 start-Turn# dN #Turns/ramp dWs/turn (MeV)
'PARTICUL'
938.27203d0 1.602176487d-19 1.7928474d0 0. 0.
'SPNTRK'
4.1
-6.8608394896E-02 0.1001299394 0.9926061069
'FAISTORE'
b_zgoubi.fai #Start
1
'SPNSTORE'
b_zgoubi.spn #Start
1
'MARKER' #Start
'MULTIPOL' SBEN ALBF
0 .Dip
200.6554 10.00 0.1171 0.0484 -0.00053604 0 0 0 0 0 0 0
0. 0. 10.00 4.0 0.800 0.00 0.00 0.00 0.00 0. 0. 0. 0.
4 .1455 2.2670 -.6395 1.1558 0. 0. 0.
0. 0. 10.00 4.0 0.800 0.00 0.00 0.00 0.00 0. 0. 0. 0.
4 .1455 2.2670 -.6395 1.1558 0. 0. 0.
0 0 0 0 0 0 0 0 0. 0. 0.
#20|200|20 Dip ALBF
3 0.0 0.0 -1.175115045E-002
.....
```

```
'MULTIPOL' SBEN I5AF
0 .Dip
238.7522 10.00 0.11712611 0.04865458 -0.00045118 0 0 0 0 0 0 0
0. 0. 10.00 4.0 0.800 0.00 0.00 0.00 0.00 0. 0. 0. 0.
4 .1455 2.2670 -.6395 1.1558 0. 0. 0.
0. 0. 10.00 4.0 0.800 0.00 0.00 0.00 0.00 0. 0. 0. 0.
4 .1455 2.2670 -.6395 1.1558 0. 0. 0.
0 0 0 0 0 0 0 0 0. 0. 0.
#20|200|20 Dip I5AF
3 0. 0. -1.398251535000000E-002
'DRIFT' DRIF D2H
76.1927
'MULTIPOL' QJUMI
! Betax, Alphas : 2.57E+01 -1.96E-01, Betax, Alphas : 8.95E+00 -8.93E-03
0 .Quad
76.1927 10.00 0.0 0.00818 0.0 0 0 0 0 0 0 0
0. 0. 6.00 3.00 1.00 0.00 0.00 0.00 0.00 0. 0. 0. 0.
6 .1122 6.2671 -1.4982 3.5882 -2.1209 1.723
0. 0. 6.00 3.00 1.00 0.00 0.00 0.00 0.00 0. 0. 0. 0.
6 .1122 6.2671 -1.4982 3.5882 -2.1209 1.723
0 0 0 0 0 0 0 0 0. 0. 0.
#30|76|30 Quad QJUMI
1 0. 0. 0.
.....
'MULTIPOL' SBEN J5AF
0 .Dip
238.7522 10.00 0.11712611 0.04865458 -0.00045118 0 0 0 0 0 0 0
0. 0. 10.00 4.0 0.800 0.00 0.00 0.00 0.00 0. 0. 0. 0.
4 .1455 2.2670 -.6395 1.1558 0. 0. 0.
0. 0. 10.00 4.0 0.800 0.00 0.00 0.00 0.00 0. 0. 0. 0.
4 .1455 2.2670 -.6395 1.1558 0. 0. 0.
0 0 0 0 0 0 0 0 0. 0. 0.
#20|200|20 Dip J5AF
3 0. 0. -1.398251535000000E-002
'DRIFT' DRIF D2H
76.1927
'MULTIPOL' QJUMJ
! 2.7xQJUMI Betax,Alphas: 2.55E+01 -1.09E-01; Betay,Alphas: 8.17E+00 3.29E-02
0 .Quad
! 3.7*kl=4pi*dQ/betx=4pi*0.04/25.6=0.01963
! b1(T)=Brho*(kl/1*2.7/3.7)*a=1*0.01963/3.7*0.1=0.001433
76.1927 10.00 0.0 0.0221 0.0 0 0 0 0 0 0 0
0. 0. 6.00 3.00 1.00 0.00 0.00 0.00 0.00 0. 0. 0. 0.
6 .1122 6.2671 -1.4982 3.5882 -2.1209 1.723
0. 0. 6.00 3.00 1.00 0.00 0.00 0.00 0.00 0. 0. 0. 0.
6 .1122 6.2671 -1.4982 3.5882 -2.1209 1.723
0 0 0 0 0 0 0 0 0. 0. 0.
#30|76|30 Quad QJUMJ
1 0. 0. 0.
.....
'DRIFT' DRIF DSG10
31.7339
'CAVITE'
2 .1 .1 is to fill zgoubi.CAVITE.Out for plot using zpop/7/20
807.042748 12. 0435
290.d3 2.617993877991494365 9cavitiesx32kV, phi_s=150deg
'MARKER' #End
'SPNRPT'
'FAISCEAU'
'REBELOTE'
19999 0.2 99
'END'
```